



# Discovery of a quinoline-containing compound JT21-25 as a potent and selective inhibitor of apoptosis signal-regulating kinase 1 (ASK1)

Lidan Pang<sup>a,1</sup>, Tiantian Wang<sup>b,1</sup>, Jiateng Huang<sup>a,1</sup>, Jie Wang<sup>a</sup>, Xiang Niu<sup>a</sup>, Hao Fan<sup>a</sup>, Pingnan Wan<sup>a,\*</sup>, Zengtao Wang<sup>a,\*</sup>

<sup>a</sup> College of Pharmacy, Jiangxi University of Chinese Medicine, Nanchang 330004, PR China

<sup>b</sup> National Pharmaceutical Engineering Center for Solid Preparation in Chinese Herbal Medicine, Jiangxi University of Chinese Medicine, Nanchang 330006, PR China

## ARTICLE INFO

### Keywords:

Synthesis  
Molecular docking  
Biological evaluation  
ASK1 inhibitors

## ABSTRACT

ASK1 kinase inhibition has become a promising strategy for treating inflammatory diseases, such as non-alcoholic steatohepatitis and multiple sclerosis. Here, we reported the discovery of a promising compound **9h** (**JT21-25**) containing quinoline structures as a potent small molecule inhibitor of ASK1. The compound **JT21-25** was selective against MAP3K kinases TAK1 (>1960.8-fold), and much higher than the selectivity of **GS-4997** for TAK1 (312.3-fold). In addition, different concentrations of **JT21-25** did not show significant toxicity in normal LO2 liver cells, and the cell survival rate was greater than 80 %. The Oil Red O staining experiment showed that at the 4  $\mu$ M and 8  $\mu$ M concentrations of **JT21-25**, only slight cytoplasmic fat droplets were observed in LO2 cells, and there was no significant fusion between fat droplets. In the biochemical analysis experiment, **JT21-25** significantly reduced the content of CHOL, LDL, TG, ALT, and AST. In summary, these findings suggested that compound **JT21-25** might be valuable for further investigation as a potential candidate in the treatment of associated diseases.

## 1. Introduction

Apoptosis signal-regulated kinase 1 (ASK1, also known as MAP3K5) is a member of the mitogen-activated protein kinase kinase kinase (MAP3K) family located upstream of Jun N-terminal kinase (JNK) and p38 [1–3]. A series of studies have shown that ASK1 responds to many stress-induced signals, such as reactive oxygen species (ROS) [4], endoplasmic reticulum (ER) stress [5], lipopolysaccharide [6,7], etc. The increase in ASK1 activity is related to various pathologies, including neurodegenerative diseases [8–11], cardiovascular diseases [12–15], liver diseases [16,17], and cancer [18,19], etc. Therefore, ASK1 has become a potential drug target, its inhibitors have been continuously discovered as important drug application compounds for treating these diseases.

In the early stage, the Ichijo group reported a potent ASK1 inhibitor **1** (**K812**, Fig. 1) containing a quinoline ring with an IC<sub>50</sub> value of 6 nM [20]. Subsequent studies showed that oral administration of **K812** significantly prolonged the lifespan of SOD1G93A transgenic mice (Animal model of amyotrophic lateral sclerosis, with a 1.08 % increase

in survival rate) [21]. Later, Gilead Sciences, Inc. synthesized an important lead compound **2** (**GS-4997**, Fig. 1), with an IC<sub>50</sub> value of 6 nM [22], which had been studied in Phase II and III clinical trials for the treatment of diabetes nephropathy [23–25] and nonalcoholic steatohepatitis [26]. In addition, it has been shown that oral administration of ASK1 inhibitor **3** (**GS-444217**, Fig. 1) could reduce pulmonary artery pressure in animal models [27]. Another selective ASK1 inhibitor **4** (**GS-627**, Fig. 1) was also discovered by Gilead and exhibited good anti-arthritis activity in collagen induced rat arthritis models [28].

At present, although there are candidate drugs that have entered clinical research, such as **GS-4997**, there are still no ASK1 inhibitors approved for the market. Most of the reported inhibitors are in the early preclinical research and biological activity evaluation stage, such as quinoxaline derivatives [29], 1*H*-indazole derivatives [30], 1*H*-indole-2-carboxamide derivatives [31], macrocyclic analogs [32], iso-indolinone derivatives [33]. Therefore, it is still necessary to develop novel ASK1 inhibitors at this stage.

Recently, our research group have developed a series of novel ASK1 inhibitors [29]. With our interest in ASK1 inhibitors, we carefully

\* Corresponding authors.

E-mail addresses: [815368291@qq.com](mailto:815368291@qq.com) (P. Wan), [zengtaowang@126.com](mailto:zengtaowang@126.com) (Z. Wang).

<sup>1</sup> These authors contributed equally to this work.

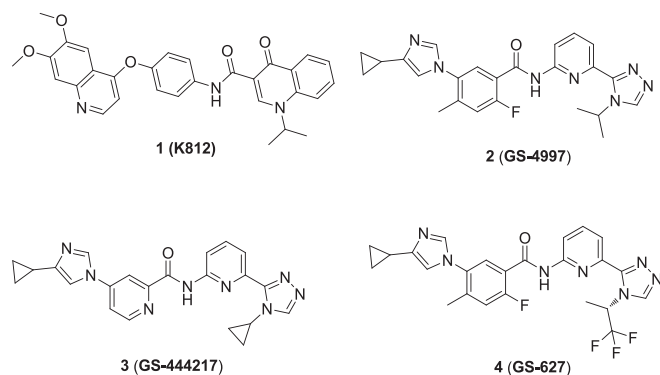


Fig. 1. Representative ASK1 small molecule inhibitors.

analyzed the molecular docking modes of GS-4997 and K812 with ASK1 protein. Compound GS-4997 occupied the ATP-binding pocket of ASK1 and interacted with the hinge binder residue (Val 757) and catalytic lysine residue (Lys 709) (Fig. 2A). While K812 formed a hydrogen bond with the hinge binder residue Val 757, it also formed a special Pi-sulfur interaction with Met 754 (Fig. 2B). In addition, the imidazole ring and quinoline ring on the left side of the structure of GS-4997 and K812 were placed in the solvent-exposed region, and the group at this position did not interact with the key amino acid residues, so the modification of the structural group here usually had little impact on the activity, and could improve the drug-like properties of the compounds. In view of the above observation and analysis, we considered modifying the imidazole

ring of GS-4997 in the solvent-exposed region, that is, the imidazole ring and benzene ring of GS-4997 were fused to introduce the quinoline aromatic heterocycle of K812 (Fig. 2C). Also, various substituents were introduced into the quinoline moiety to investigate the effect on inhibitory activity, and a comprehensive structure-activity relationship (SAR) study was conducted, including the research on the inhibitory effects of modifying moieties B and C. The detailed design strategy is shown in Fig. 2. In this study, we will synthesize a series of quinoline compounds, and study their ASK1 inhibitory activity, selectivity, cytotoxicity, cellular fatty liver efficacy, molecular docking, and ADME properties.

## 2. Results and discussions

### 2.1. Chemistry

The preparation of the title compounds 9a-9h and 10a-10d is shown in Scheme 1. The acyl hydrazine 6 was obtained in a higher yield by using methyl 6-aminopicolinate (5) and hydrazine hydrate in MeOH at reflux, and then reacted with 1, 1-dimethoxy-*N*, *N*-dimethylmethanamine (DMF-DMA) to afford compound 7 with a yield of 65 %. The resulting 7 is further reacted with isopropylamine in the presence of AcOH/MeCN to give triazole product 8 in moderate yield. Under 1-propanephosphonic acid cyclic anhydride (T3P) and triethylamine (Et<sub>3</sub>N) or 1-ethyl-3-(3-dimethylpropylamine) carbodiimide (EDCI) and *N*-hydroxysuccinimide (NHS) conditions, compound 8 was treated with the corresponding aromatic acids to obtain amide product 9a-9h. Finally, the Suzuki cross-coupling reaction of 9e-9h with the 1-methyl-4-(4, 4, 5, 5-

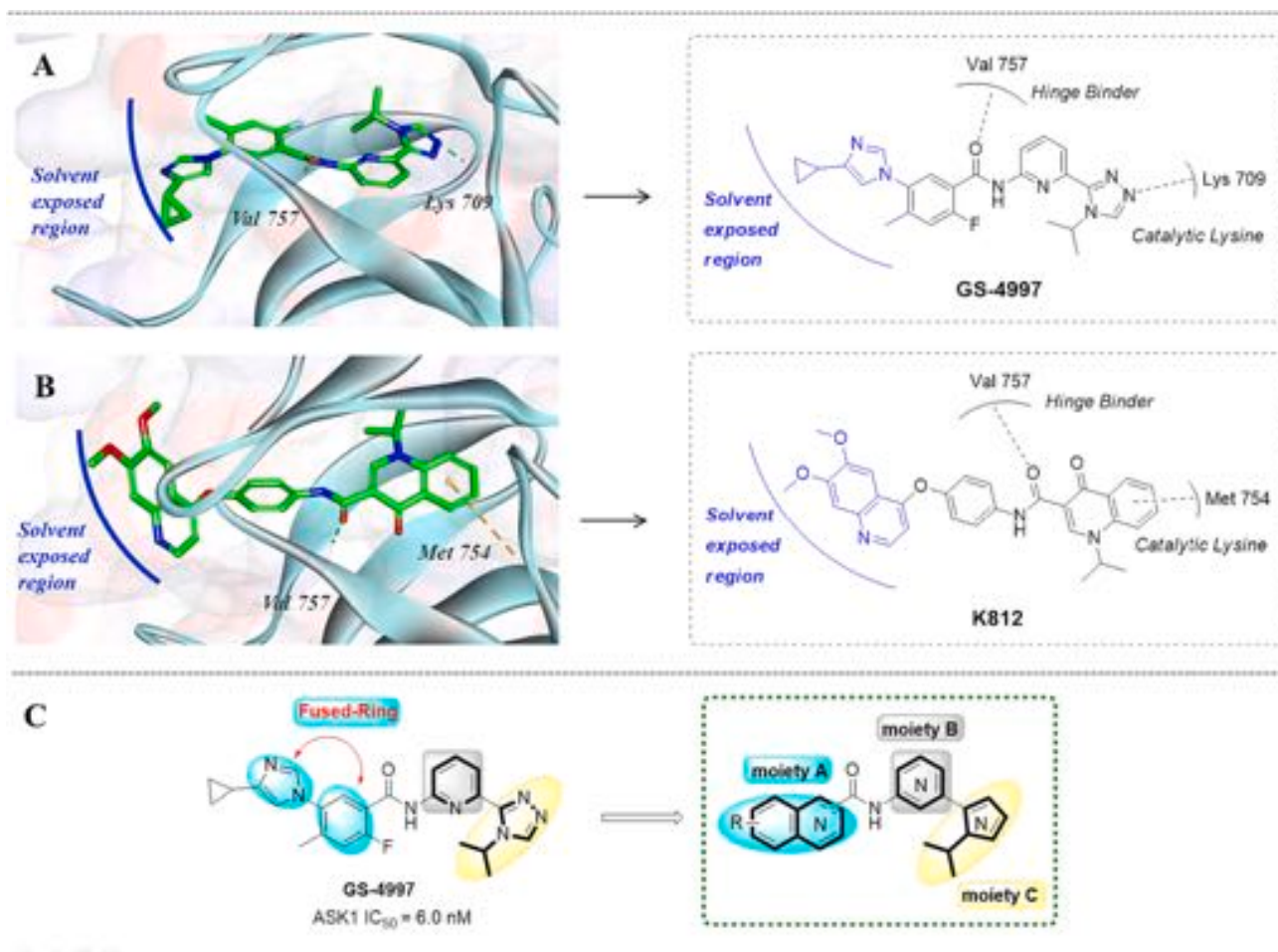
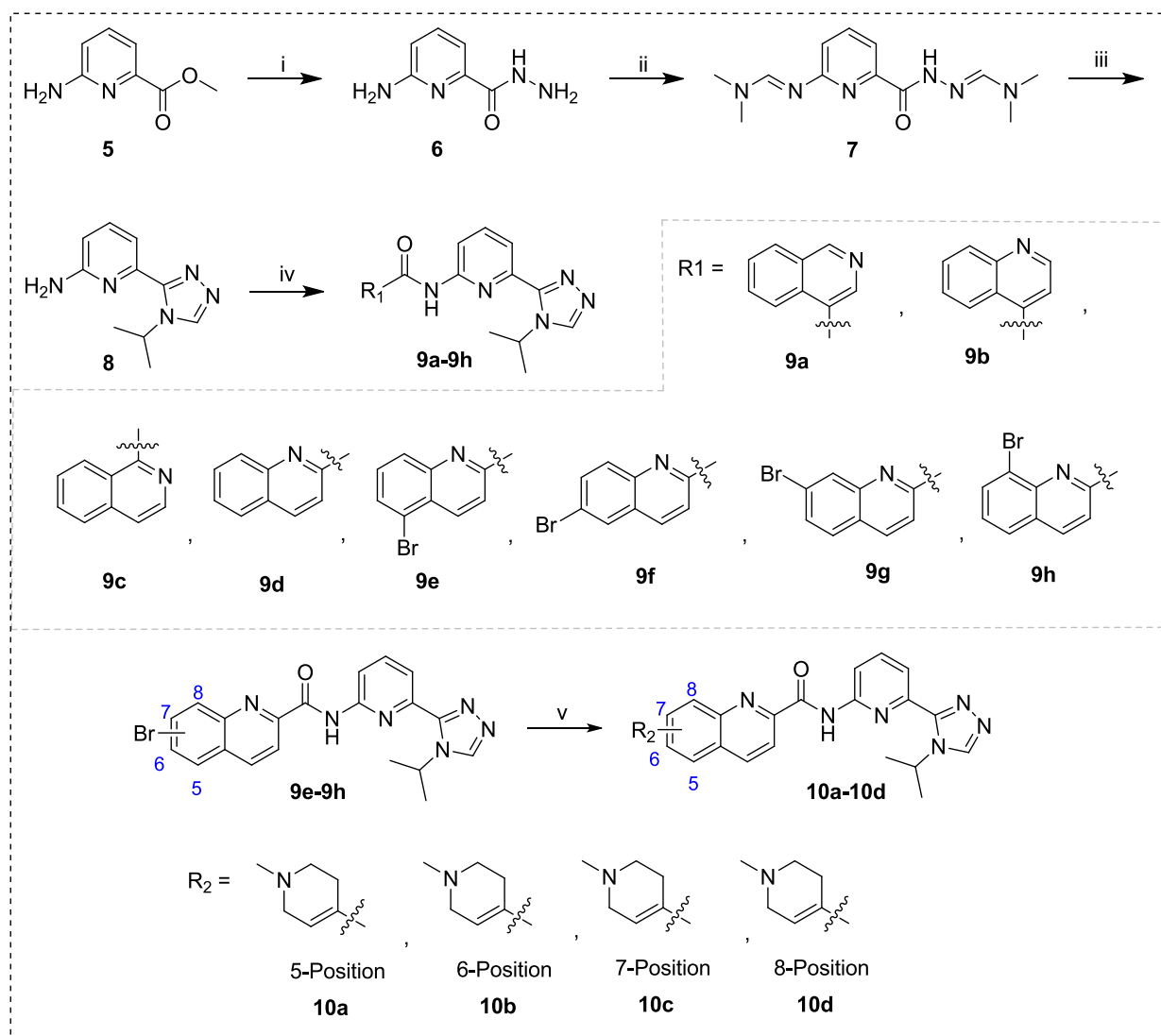


Fig. 2. Binding mode of compounds GS-4997 and K812 bound to ASK1 (PDB code: 5UOX) and optimization strategy.



**Scheme 1.** Synthesis of title compounds **9a-9h**, and **10a-10d**. Reagents and conditions: (i) Hydrazine hydrate (2.0 eq.), MeOH, reflux, 7h, 95 % yield; (ii) DMF-DMA, reflux, 3 h, 65 % yield; (iii) isopropylamine (5 eq.), AcOH (3 eq.), MeCN, 90 °C, 16 h, 51.3 % yield; (iv) **9a**, **9b**, **9e-9h** for a: corresponding aromatic acids (1.0 eq.),  $T_3P$  (4.0 eq.), Et<sub>3</sub>N (7.0 eq.), CH<sub>2</sub>Cl<sub>2</sub>, rt., 24 h, 25.8–55.2 % yield; **9c**, **9d** for b: corresponding aromatic acids (1.0 eq.), EDCI (1.0 eq.), NHS (1.0 eq.), CH<sub>2</sub>Cl<sub>2</sub>, rt., 24 h, 23.7 %–26.6 % yield; (v) Na<sub>2</sub>CO<sub>3</sub> (5 eq.), Pd(PPh<sub>3</sub>)<sub>4</sub> (0.1 eq.); DME/H<sub>2</sub>O (1:1, v/v), 80 °C, 2 h, 50.5–99.5 % yield.

tetramethyl-1, 3, 2-dioxaborolan-2-yl)-1, 2, 3, 6-tetrahydropyridine provided title molecules **10a-10d** with a range of 50.5–99.5 % yield.

As depicted in [Scheme 2](#), the amide products **15a-15e** were prepared in a similar way to the above [Scheme 1](#). In addition, the preparation of the title compounds **18a-18f** and **19** was shown in [Scheme 3](#). The Suzuki cross-coupling reaction of 6-bromopyridin-2-amine (**16**) with 1-isopropyl-5-(4, 4, 5, 5-tetramethyl-1, 3, 2-dioxaborolan-2-yl)-1*a*-pyrazole generated intermediate **17a**, subsequent amide bond formation *via* reaction with **17a** and commercially available 2-quinolinecarboxylic acid produced amide **18a** in 75.6 %. Different substituted triazole intermediates **17b-17f** were synthesized from **7** using a synthesis procedure similar to that of **8**. The obtained **17b-17f** and 2-quinolinecarboxylic acid or 8-bromoquinoline-2-carboxylic acid were then used as the reaction raw material to prepare the final product **18b-18f** and **19** under two different reaction conditions, including the acyl chloride method and the POCl<sub>3</sub> method.

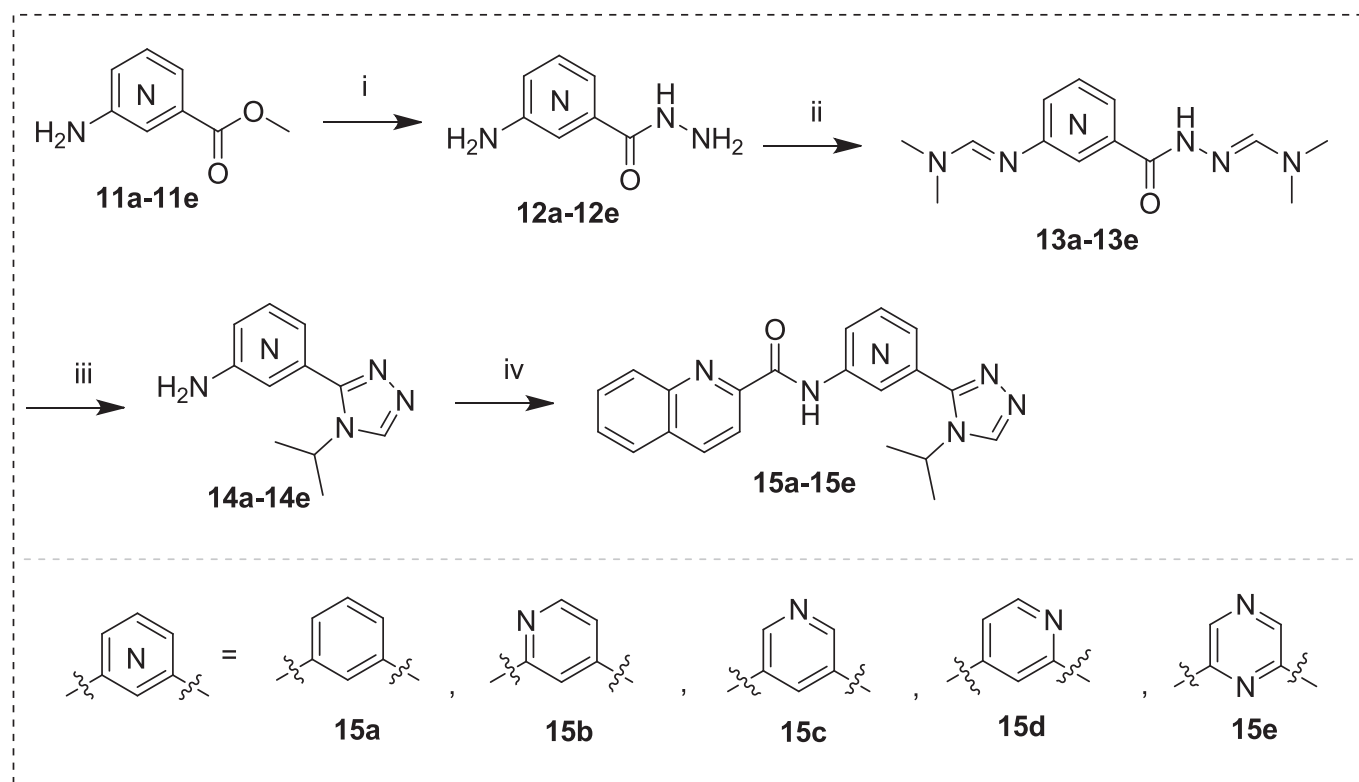
## 2.2. Biological evaluation

### 2.2.1. Inhibitory activity against ASK1

In this study, to explore and discover new small molecule inhibitors

of ASK1 protein, we performed a comprehensive structural modification and structure–activity relationship study from the moiety A-C three parts of the inhibitors. The *in vitro* ASK1 kinase inhibitory activities of all synthesized target products were shown in [Tables 1-3](#), and the results of kinase selectivity experiments were shown in [Table 4](#). Firstly, we explored the effect of quinoline or isoquinoline compounds **9a-9d** with different *N*-substituted positions on their activity. The inhibitory activity sequence was **9d** > **9c** > **9b** > **9a** ([Table 1](#)). The 2-substituted quinoline skeleton product **9d** showed potent inhibitory activity, with an IC<sub>50</sub> value of up to 25 nM. In addition, the inhibitory activity of 1-substituted isoquinoline product **9c** was 889 nM, that of 4-substituted isoquinoline product **9b** was 5705 nM, and that of 4-substituted isoquinoline product **9a** was more than 10000 nM. The activities of the above compounds exhibited significant differences due to their different structures.

In order to further optimize compound **9d**, a detailed SAR study was conducted based on its *in vitro* ASK1 kinase activity. The solvent-exposed region was explored by introducing substituent groups at different positions of the quinoline ring. The brominated products **9e-9g** with different substitution positions and nitrogen-containing heterocyclic 1-methyl-1, 2, 3, 6-tetrahydropyridine products **10a-10d** were further synthesized and evaluated in ASK1 kinase assays. Among the



**Scheme 2.** Synthesis of target compounds **15a-15f**. Reagents and conditions: (i) Hydrazine hydrate (2.0 eq.), MeOH, reflux, 7 h, 95–100 % yield; (ii) DMF-DMA, reflux, 3 h, 53.2–73 % yield; (iii) isopropylamine (5 eq.), AcOH (3 eq.), MeCN, 90 °C, 16 h, 17.6–56.5 % yield; (iv) POCl<sub>3</sub> (4.0 eq.), pyridine, rt., 2 h, 30.7–57.9 % yield.

brominated products, 8-bromo substituted quinoline product **9h** (**JT21-25**) exhibited the most potent inhibitory activity with an IC<sub>50</sub> of 5.1 nM. Other substituted positions, such as bromination at 5-position, or 6-position, or 7-position, led to slightly decreased ASK1 kinase activity (**9e-9g**), and their IC<sub>50</sub> values were within the range of 20–55 nM. Interestingly, in the subsequent assays of alkaline nitrogen heterocyclic coupling products, it was found that the 5-substituted 1-methyl-1, 2, 3, 6-tetrahydropyridine product **10a** exhibited the best inhibitory activity, with an IC<sub>50</sub> of 21.2 nM (Table 1). However, the replacement of the bromine group with 1-methyl-1, 2, 3, 6-tetrahydropyridine (**10d**) at 5-position led to significantly decreased ASK1 kinase activity, with an ASK1 IC<sub>50</sub> of 2432.5 nM, which was approximately 477 times lower than **JT21-25**.

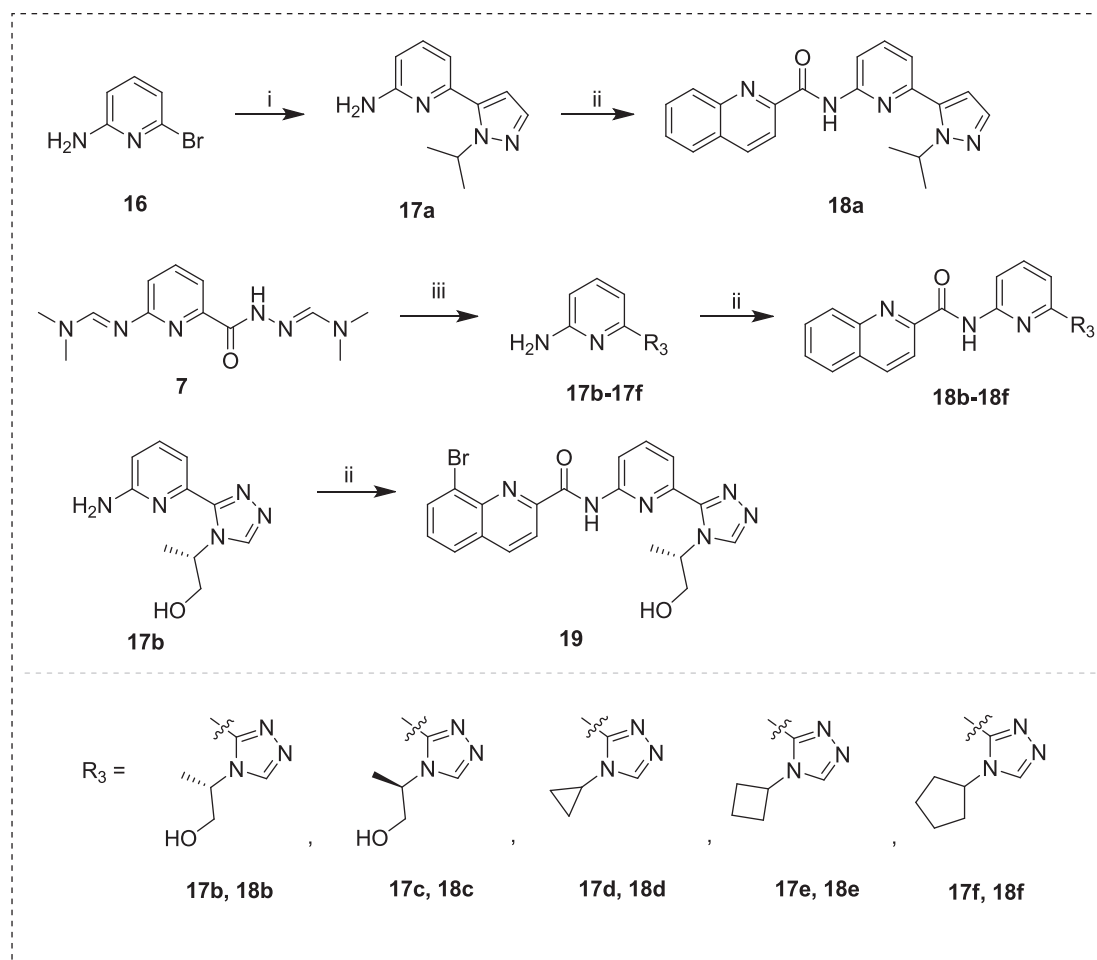
Subsequently, we further optimized the structure of compound **9d** and investigated the structure–activity relationship of its moiety B. The modification strategy was to replace the pyridine ring in moiety B with a benzene ring (**15a**), pyridine ring nitrogen at different nitrogen atom positions (**15b-15d**), and a piperazine ring containing two nitrogen atoms (**15e**). These modified compounds were tested for ASK1 kinase inhibitory activity, as shown in Table 2. Compared with compound **9a**, **15a** lacking the nitrogen atom of the pyridine ring showed a significant decrease in ASK1 inhibitory activity (IC<sub>50</sub> = 4553.6 nM), which was approximately 182 times lower. In addition, changing the position of nitrogen atoms in the pyridine ring structure resulted in a loss of inhibitory activity of the compound (**15b-15d**, IC<sub>50</sub> > 10000 nM). These research results indicated that the presence or different positions of nitrogen atoms in moiety B had a significant impact on the inhibitory activity of the inhibitors. Interestingly, when we kept the nitrogen atom in moiety B unchanged and added an additional nitrogen atom to form a piperazine ring, its inhibitory activity still showed a significant decrease (**15e**, IC<sub>50</sub> = 1407 nM).

Finally, we focused on investigating the structure–activity relationship of moiety C by introducing pyrazole rings, (S)-2-triazolyl-propan-1-

ol, and (R)-2-triazolyl-propan-1-ol to replace the 4-isopropyl-triazolyl of **9d**. At the same time, we cyclized the isopropyl of **9d**, and introduced a three-membered ring, four-membered ring, and five-membered ring, respectively. Among these compounds, we found that the introduction of pyrazole resulted in a loss of enzyme inhibitory activity. Interestingly, enantiomer products **18b** and **18c** showed obvious differences in inhibitory activity, such as the IC<sub>50</sub> of S-isomer **18b** reaches 9.7 nM, while the inhibitory activity of R-isomer **18c** is 213.1 nM, which is nearly 22-fold different. In the subsequent isopropyl product optimization, we found that the five-membered ring **18f** had the best activity, with an IC<sub>50</sub> of 14.9 nM, followed by the three-membered ring and four-membered ring products, with inhibitory activities of 61.6 nM and 188.2 nM, respectively. Given the results of previous structure–activity relationship studies, we knew that 8-brominated product **9h** exhibited potent inhibitory activity, with an IC<sub>50</sub> of up to 5.1 nM. Therefore, we considered introducing 8-bromine into the structure of the more active S-isomer product **18b**, and obtained product **19**. The inhibitory activity against ASK1 of compound **19** reached 10.2 nM, but it was not more active than **18b**.

To evaluate the kinase selectivity of quinolone-containing compounds, we tested potent ASK1 inhibitors **9e-9g**, **JT21-25**, **10a** and **10b** in TAK1 (MAP3K7) kinase assay, where TAK1 kinase together with ASK1 are members of the MAP3K kinase family (Table 4). Simultaneously, **GS-4997** was also tested as a positive control drug.

Compound **JT21-25** was identified as the most potent ASK1 inhibitor (IC<sub>50</sub> = 5.1 nM) and it exhibited the highest selectivity for ASK1 against TAK1 (>1960.8-fold) in this series. For comparison, the inhibitory activity of **JT21-25** was slightly higher than that of **GS-4997** (IC<sub>50</sub> = 6.0 nM), while the selectivity for ASK1 against TAK1 was much higher than that of **GS-4997** (312.3-fold). Among others, compounds **9e-9g**, **10a** and **10b** were also prepared, but they inhibited ASK1 and TAK1 with IC<sub>50</sub> values in a close range. Interestingly, the inhibition of TAK1 by **10a** (IC<sub>50</sub> = 5.7 nM) has a more potent inhibitory activity than ASK1, with



**Scheme 3.** Synthesis of target compounds **18a–18f**. Reagents and conditions: (i) Xphos-Pd-G<sub>2</sub> (0.1 eq.), Na<sub>2</sub>CO<sub>3</sub> (10 eq.), dioxane:H<sub>2</sub>O = 5:1, 100 °C, 2 h, 51.3 % yield; (ii) **18b**, **18c**, **19** for a: SOCl<sub>2</sub> (2.4 eq.), DIPEA (2 eq.), toluene, 19.0–26.7 % yield; **18a**, **18d–18f** for b: POCl<sub>3</sub> (4.0 eq.), pyridine, rt., 2 h, 74.9–96.4 % yield; (iii) amines (5 eq.), AcOH (3 eq.), MeCN, 90 °C, 16 h, 17.6–79.5 % yield.

approximately 4-fold selectivity for TAK1 against ASK1. Therefore, **10a** was considered as a good molecular template and lead compound for the development of TAK1 inhibitors, which have recently been reported to have important applications in the treatment of inflammatory diseases [34,35] and KRAS mutant colorectal cancer growth [36]. Overall, we obtained a potent and selective ASK1 inhibitor **JT21-25** for the next stage evaluations.

### 2.2.2. Kinase selectivity of **JT21-25**

A kinase selectivity profiling study was conducted against a panel of 41 kinases at 1  $\mu$ M to evaluate the target selectivity of compound **JT21-25**. As shown in Fig. 3, compound **JT21-25** did not show significant inhibitory effect on the kinome (inhibition > 90 %, Table S1), and the absolute majority of kinase inhibition rates were below 50 %. This result indicates that **JT21-25** has good target selectivity, making it a promising candidate for further development as an ASK1 inhibitor.

### 2.2.3. Cytotoxicity assessment

To further demonstrate the advantages of potent **JT21-25**, we evaluated the cytotoxicity of compound **JT21-25** against LO2 cells (Fig. 4). Different concentrations of compounds **JT21-25** and **GS-4997** (0.05, 0.1, 0.4, 0.8, and 1  $\mu$ M) were incubated together with LO2 cells. **GS-4997** is used as a positive control drug. It should be noted that the cell survival rate of **JT21-25** is higher than 80 % at different concentrations, especially at low concentrations of 0.05 and 0.1  $\mu$ M, the cell survival rate of **JT21-25** was higher than that of **GS-4997**. In a word, these results indicated that compound **JT21-25** had good safety even at high

concentrations in normal human liver cells.

### 2.2.4. hERG patch clamp assay

As a further safety assessment, we evaluated the inhibitory effect of hERG. The inhibition of hERG encoded cardiac potassium channels is frequently associated with QT interval prolongation and life-threatening arrhythmias [37,38]. Therefore, early and effective prediction, evaluation, and optimization to avoid the inhibitory activity of drugs on hERG potassium channels can help reduce the cost of drug development and improve the success rate of drug development.

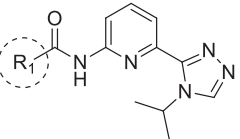
In this article, we tested the ability of **JT21-25** to inhibit hERG potassium channels. Firstly, we recorded the hERG current using whole cell patch clamp technology at a holding potential of  $-80$  mV, and then depolarized to  $-50$  mV for 0.5 s to test for leak current. Then we depolarized the voltage to 30 mV for 2.5 s. The peak tail current was induced by a repolarizing pulse to  $-50$  mV for 4 s. Repeated the protocol at 10 s intervals to observe the effect of the test substance on the tail current of Herg. The time courses of hERG currents after application of **JT21-25** at a concentration of 10  $\mu$ M were shown in Fig. 5A, and the representative traces of hERG currents before and after the application of **JT21-25** at a concentration of 10  $\mu$ M were shown in Fig. 5B. The results showed that the inhibitory rate of **JT21-25** at a concentration of 10  $\mu$ M was 7.48 %, exhibiting marginal inhibitory activities with an IC<sub>50</sub> exceeding 10  $\mu$ M.

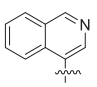
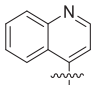
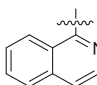
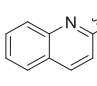
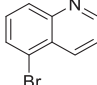
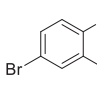
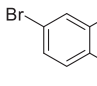
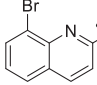
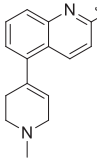
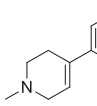
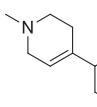
### 2.2.5. Oil Red O staining

To simulate the NAFLD phenotype, LO2 cells were treated with FFA

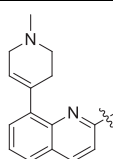


**Table 1**  
Inhibitory activity of compounds **9a-9h** and **10a-10d** against

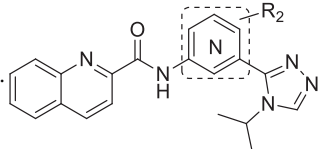
ASK1. 

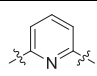
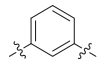
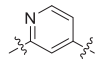
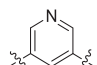
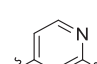
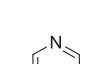
Compounds	R <sub>1</sub>	Inhibition rate <sup>a</sup> (10 μM)	IC <sub>50</sub> <sup>b</sup> (nM)
<b>9a</b>		17.5 ± 6.0	>10000
<b>9b</b>		73.2 ± 2.8	5705
<b>9c</b>		89.8 ± 1.7	889
<b>9d</b>		99.1 ± 0.5	25.0
<b>9e</b>		97.9 ± 0.4	55.0
<b>9f</b>		98.2 ± 1.0	20.2
<b>9g</b>		97.1 ± 0.2	36.0
<b>9h (JT21-25)</b>		99.6 ± 0.7	5.1
<b>10a</b>		99.0 ± 0.0	21.2
<b>10b</b>		99.3 ± 0.2	32.4
<b>10c</b>		92.9 ± 1.8	116.0

**Table 1 (continued)**

Compounds	R <sub>1</sub>	Inhibition rate <sup>a</sup> (10 μM)	IC <sub>50</sub> <sup>b</sup> (nM)
<b>10d</b>		86.3 ± 1.6	2432.5

<sup>a</sup> The values were from at least two independent experiments.<sup>b</sup> ASK1 IC<sub>50</sub> values were determined by using an ADP-Glo™ Kinase Assay as a single independent experiment.**Table 2**  
Inhibitory activity of compounds **15a-15d** against

ASK1. 

Compounds	R <sub>2</sub>	Inhibition rate <sup>a</sup> (10 μM)	IC <sub>50</sub> <sup>b</sup> (nM)
<b>9d</b>		99.1 ± 0.5	25.0
<b>15a</b>		50.9 ± 1.7	4553.6
<b>15b</b>		−8.6 ± 3.4	>10000
<b>15c</b>		48.4 ± 1.8	>10000
<b>15d</b>		16.3 ± 2.2	>10000
<b>15e</b>		71.6 ± 1.3	1407.0

<sup>a</sup> The values were from at least two independent experiments.<sup>b</sup> ASK1 IC<sub>50</sub> values were determined by using an ADP-Glo™ Kinase Assay as a single independent experiment.

for 24 h. As expected, Oil Red O staining showed that the LO2 cells in the normal control group have clear edge, abundant cytoplasm, intact nuclear membrane, large nucleus, and there are no lipid droplets inside the cell (Fig. 6a). In the FFA group, steatosis cells can be seen, and a large number of red lipid droplets in the cytoplasm were fused, accompanied by the fusion of lipid droplets (Fig. 6b). Compared with the FFA group, cytoplasmic fat droplets were reduced, but there was no significant fusion between fat droplets in LO2 cells after treatment with 1 μM JT21-25 + 1 mM FFA (Fig. 6c). In the 4 μM JT21-25 + 1 mM FFA and 8 μM JT21-25 + 1 mM FFA treatment group, only slightly cytoplasmic fat droplets were seen (Fig. 6d and 6e). The same result can be observed in Fig. 7A, FFA-induced lipid accumulation in LO2 cells was quite obvious (204 %), and JT21-25 at different concentrations significantly inhibited FFA-induced lipid accumulation in LO2 cells from 186 % to 150 %.

**Table 3**  
Inhibitory activity of compounds **18a-18f** against

ASK1.				
Compounds	X	R <sub>3</sub>	Inhibition rate <sup>a</sup> (10 μM)	IC <sub>50</sub> <sup>b</sup> (nM)
<b>9d</b>	H		99.1 ± 0.5	25.0
<b>18a</b>	H		7.2 ± 2.9	>10000
<b>18b</b>	H		98.8 ± 0.03	9.7
<b>18c</b>	H		92.5 ± 0.3	213.1
<b>18d</b>	H		99.2 ± 0.6	61.6
<b>18e</b>	H		96.5 ± 0.1	188.2
<b>18f</b>	H		99.1 ± 0.2	14.9
<b>19</b>	Br		98.6 ± 0.5	10.2

<sup>a</sup> The values were from at least two independent experiments.<sup>b</sup> ASK1 IC<sub>50</sub> values were determined by using an ADP-Glo™ Kinase Assay as a single independent experiment.**Table 4**  
ASK1/TAK1 selectivities of selected compounds..

Compounds	ASK1 IC <sub>50</sub> <sup>a</sup> (nM)	TAK1 IC <sub>50</sub> <sup>a</sup> (nM)	Selectivity in-fold
<b>9e</b>	55.0	68.8	1.3
<b>9f</b>	20.2	37.5	1.9
<b>9g</b>	36.0	59.3	1.6
<b>JT21-25</b>	5.1	> 10,000	> 1960.8
<b>10a</b>	21.2	5.7	0.3
<b>10b</b>	32.4	74.3	2.3
<b>GS-4997</b>	6.0	1874	312.3

<sup>a</sup> IC<sub>50</sub> values were determined by using an ADP-Glo™ Kinase Assay as a single independent experiment.

### 2.2.6. Effects of JT21-25 on CHOL, LDL, TG, AST and ALT content in LO2 cells

As shown in Fig. 7B, 7C, and 7D, compared with the control group, the FFA (Free Fatty Acid) group showed significant increases in cholesterol (CHOL), low-density lipoprotein (LDL), and triglyceride (TG) levels ( $p < 0.01$  or  $p < 0.001$ ), indicating that our cell model of non-alcoholic fatty liver (NAFL) was successful. In addition, compared with the FFA group, the CHOL, LDL, and TG contents of the JT21-25 group with different concentrations were all reduced. Especially, the LDL content of JT21-25 groups with different concentrations was significantly decreased ( $p < 0.05$ , 1 μM and 8 μM or  $p < 0.01$ , 4 μM). In addition, the TG contents in 4 μM of JT21-25 also showed a significant decrease ( $p < 0.05$ ). Although the CHOL content in the FFA group slightly increased compared to the control group, the CHOL concentration in the JT21-25 group showed a significant decrease ( $p < 0.01$ ).

Meanwhile, compared with the control group, the FFA group showed an increase of 35.76 % in ALT and 22.97 % in AST levels, respectively. However, the JT21-25 groups with 1 μM and 8 μM showed a decreasing trend, especially the JT21-25 group with 4 μM concentration showed a significant decrease in ALT and AST levels ( $p < 0.05$ ) (Fig. 7E, 7F, Table 5). Unexpectedly, JT21-25 weakened its inhibitory effect on CHOL, LDL, TG, AST, and ALT levels in LO2 cells at the highest concentration, and the possible specific mechanism needs further research and verification. Anyway, it is worth noting that all of these results indicate that JT21-25 can reduce the content of CHOL, LDL, TG, ALT, and AST in FFA-induced LO2 cells, thus having the potential to treat non-alcoholic fatty disease.

### 2.2.7. Flow cytometry analysis of cell cycle distribution

In addition, we compared the cell cycle effects of compounds JT21-25 and GS-4997 (Fig. 8). HepG2 cells were treated with compounds JT21-25 and GS-4997 at indicated doses for 24 h. The cell cycle distribution was then analyzed by flow cytometry. The preliminary results showed that it was dose-dependent as the concentration increased, the percentage of HepG2 cells in the G2 phase was enhanced in the presence of GS-4997 and JT21-25. In particular, JT21-25 showed the most potent arrest effect at 16 μM among all experimental samples. The above results showed that both JT21-25 and GS-4997 could induce G2 cell cycle arrest.

### 2.3. Molecular docking

To better understand the possible molecular interaction between inhibitors and ASK1 protein (PDB code: 5UOX) [33], a representative molecule JT21-25 and control drug GS-4997 were developed using Discovery Studio version 4.5 to dock with ASK1 protein, respectively. As shown in Fig. 9 and Fig. 10, the docking research results confirmed that JT21-25 and GS-4997 had the same hydrogen bonding mode, and they had two key hydrogen bonding interactions, namely the formation of hydrogen bonds between the carbonyl group of the amide and the main chain NH of Val757, and the formation of hydrogen bonds between N1 triazole nitrogen and catalytic Lys709. Among them, Lys709 residue was located at the catalytic active center of ASK1 protein, and formed hydrogen bond with triazole fragment of ligands, resulting in potent inhibitory activity. Also, Val757 was located in the hinge region of ASK1 protein, formed hydrogen bond with the amide moiety of the ligand, thereby limiting the binding conformation of ligands and stabilizing the binding between the ligand and the active site pocket. In addition, the pyridine ring of JT21-25 and GS-4997 was responsible for forming four pi-alkyl interactions with LEU810, VAL694, VAL707 and VAL738, and a pi-sigma interaction with amino acid residues MET754, respectively.

The difference was that the quinoline ring of JT21-25 in the solvent-exposed region of the binding pocket was responsible for forming two pi-alkyl interactions with ALA764 and LEU686, respectively. In addition to forming a pi-alkyl interaction with the residue LEU686, the benzene and imidazole rings of GS-4997 at this position also formed a pi-donor

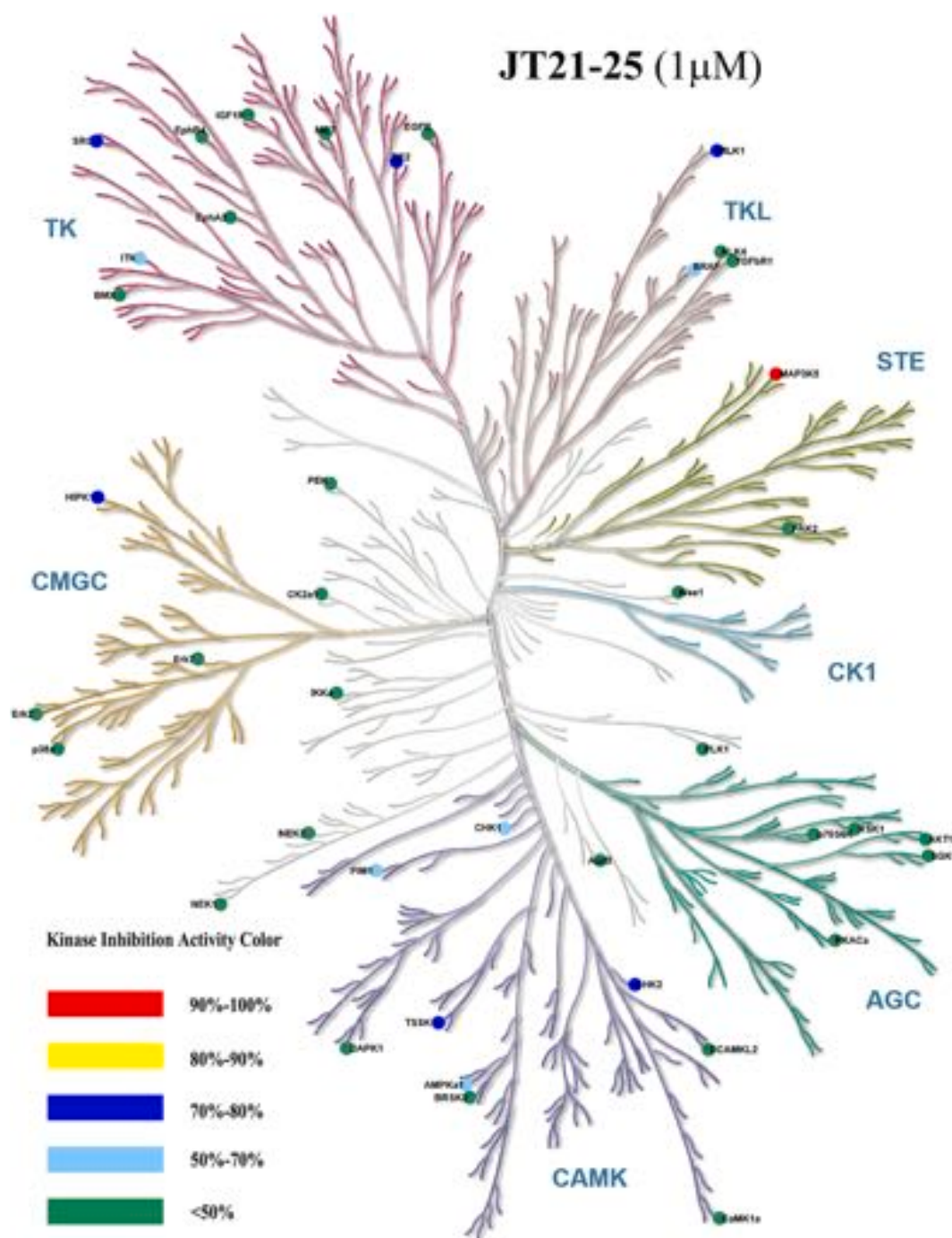


Fig. 3. Kinase inhibition profile of JT21-25 at a concentration of 1  $\mu$ M against 41 kinases.

hydrogen bond and a carbon-hydrogen bond with GLY759 and GLN756, respectively, and an alkyl bond with PRO758. However, compared to JT21-25, and GS-4997 lacked a  $\pi$  - alkyl interaction with ALA764 (Fig. 10). The results of these docking studies indicated that the binding modes of JT21-25 and GS-4997 were slightly different.

To explore the possible reasons for the high selectivity of JT21-25 against TAK1, we conducted a molecular docking study with JT21-25 and TAK1 protein (Fig. 11). The docking results revealed that JT21-25 did not form firm hydrogen bonds with TAK1 protein. On the contrary, the key triazole active fragment did not extend into the ATP-binding pocket of TAK1, but was in the solvent-exposed region. Besides, the quinolone fragment of JT21-25 only formed a weak Pi-sulfur interaction with the residue Met104, which made JT21-25 unable to bind the TAK1

active pocket stably, and resulting in no inhibitory activity against TAK1.

#### 2.4. Theoretical prediction of the ADME properties

In order to study the drug like properties of compound JT21-25, we used the SwissADME network tool to evaluate its ADME properties. As shown in Table 6, compound JT21-25 meets the requirements of Lipinski's and Veber's rules, and its structure does not contain any characteristic structural elements of pan-assay interference compounds (PAINS), indicating that the target compound JT21-25 had drug-likeness properties.



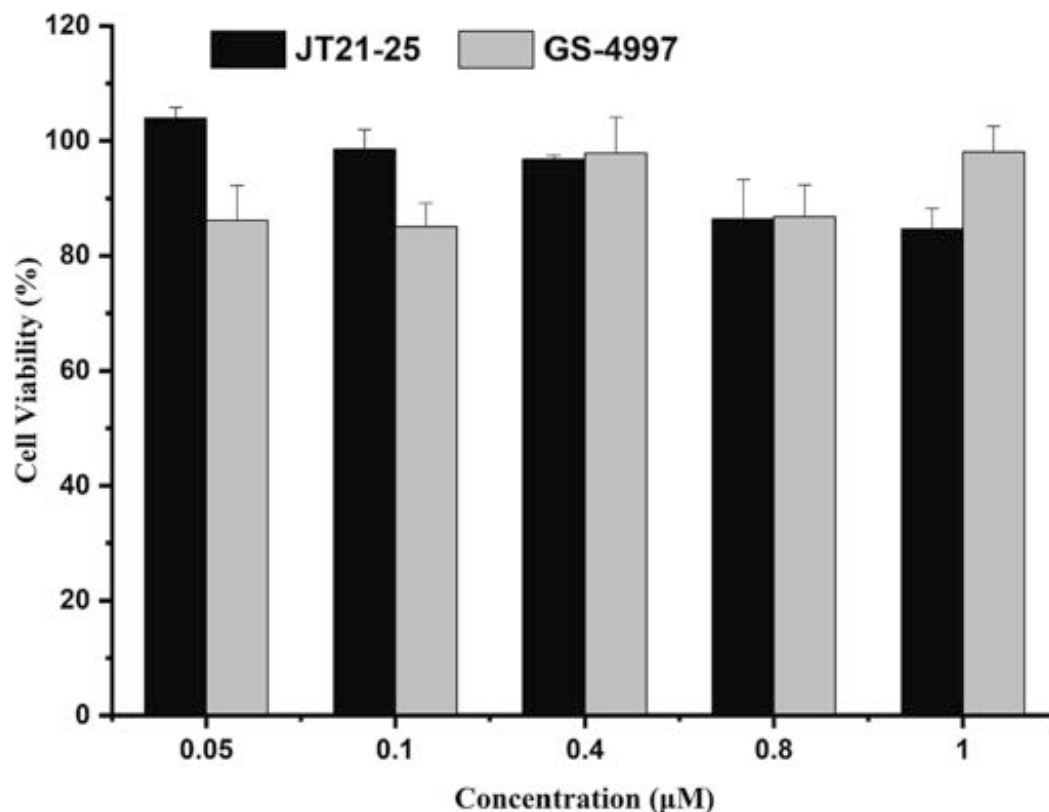


Fig. 4. Cell viability assessed by the CCK-8 assay in 24-h human normal liver LO2 cells cultures. The columns represent the mean  $\pm$  standard deviation ( $n = 6$ ). JT21-25 had better cell viability at low concentrations of 0.05 and 0.1  $\mu\text{M}$ , with a slight difference from GS-4997.

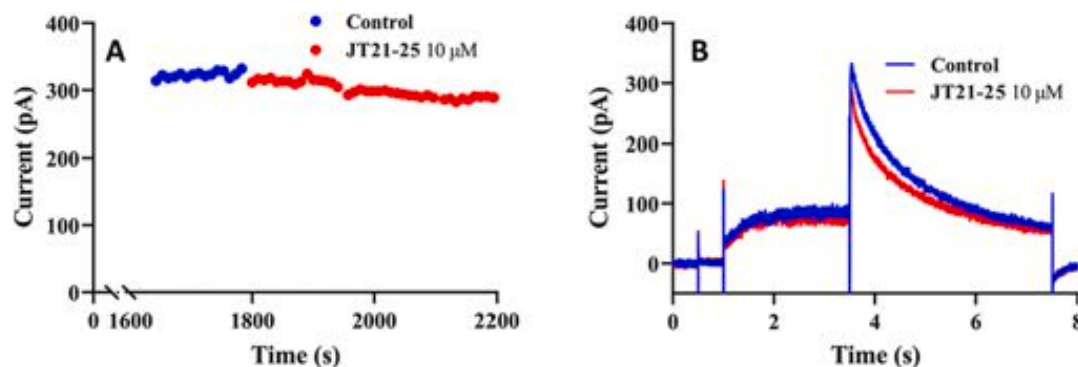


Fig. 5. The time courses and representative traces of hERG currents. (A): The time courses of hERG currents after application of JT21-25 with a concentration of 10  $\mu\text{M}$ ; (B): Representative traces of hERG currents, before and after JT21-25 application at concentration of 10  $\mu\text{M}$ .

### 3. Conclusions

In this study, a series of quinoline derivatives were designed, synthesized, and evaluated as a new structural chemotype of ASK1 inhibitors. Compound **9h** (JT21-25) exhibited the most potent ASK1 inhibitory activity and high selectivity against MAP3K kinase TAK1, with both inhibitory activity and selectivity superior to GS-4997. In addition, JT21-25 did not show significant toxicity in normal LO2 liver cells. Further Oil Red O staining experiments showed that at a concentration of 4  $\mu\text{M}$  and 8  $\mu\text{M}$ , only slight cytoplasmic fat droplets were observed in LO2 cells of JT21-25 group. The biochemical analysis results showed that JT21-25 significantly reduced the content of CHOL, LDL, TG, ALT, and AST. In summary, the ASK1 inhibitors reported in this article constitute attractive tool compounds to support elucidating the pharmacological consequences of ASK1 inhibition.

### 4. Experimental

#### 4.1. General methods

All chemicals, reagents, and solvents were purchased from Anhui Zesheng Technology Co., Ltd. and Bide Pharmatech Co., Ltd.. The infrared spectrum was recorded in KBr with a FT-IR Affinity-1 spectrophotometer, Shimadzu (Kyoto, Japan). The  $^1\text{H}$  NMR and  $^{13}\text{C}$  NMR spectrums were measured on a Bruker Avance 400 MHz NMR spectrometer. The chemical shift value is in Hertz. The split mode is expressed as s, singlet; d, doublet; t, triplets; m, multiplet; dd, doublet of  $^1\text{H}$  NMR data.

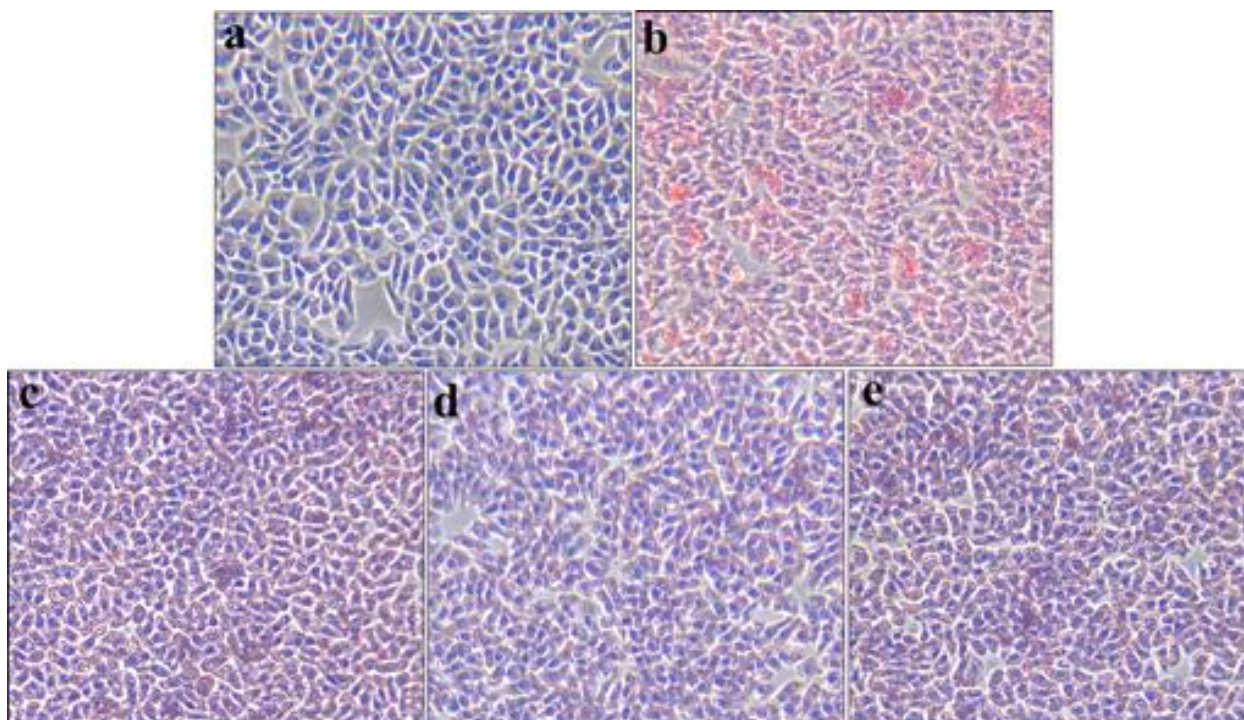


**Fig. 6.** Effect of JT21-25 on the content of lipid droplets under light microscopy in LO2 cells (a: normal control group; b: oleic acid-induced fatty liver model group; c: JT21-25 group of 1  $\mu$ M; d: JT21-25 group of 4  $\mu$ M; e: JT21-25 group of 8  $\mu$ M) (10 $\times$ 20).

#### 4.2. Synthesis of key intermediates and final compounds

**6-aminopicolino-hydrazide (6).** To a solution of methyl 6-aminopicolinate (**5**, 500 mg, 3.3 mmol) in  $\text{CH}_3\text{OH}$  (10 mL) was added hydrazine hydrate (330 mg, 6.6 mmol), the mixture was stirred at 75  $^\circ\text{C}$  for 7 h, the reaction was monitored by TLC. Upon completion, the reaction mixture was cooled to rt. The precipitate formed in the mixture was collected by filtration, washed with EA and then dried in vacuo to give **6** (475 mg, 95 % yield) as white solid.  $^1\text{H}$  NMR (400 MHz,  $\text{DMSO}-d_6$ ):  $\delta$  9.16 (s, 1H), 7.51 (dd,  $J$  = 8.4, 7.7 Hz, 1H), 7.10 (dd,  $J$  = 7.2, 0.8 Hz, 1H), 6.60 (dd,  $J$  = 8.4, 0.8 Hz, 1H), 6.10 (s, 2H), 4.51 (s, 2H); ESI-HRMS ( $m/z$ ) [ $M + H$ ] $^+$  calcd for  $\text{C}_6\text{H}_8\text{N}_4\text{O}$ , 153.0698, found 153.0776.

**6-(4-isopropyl-4H-1, 2, 4-triazol-3-yl) pyridin-2-amine (8).** A mixture of **6** (475 mg, 3.1 mmol) in 1,1-dimethoxy- $N,N$ -dimethylmethanamine (DMF-DMA) was heated under reflux for 3 h, the reaction was monitored by TLC. Upon completion, the reaction mixture was cooled to rt, and then concentrated under reduced pressure. The residue was taken up in EA (100 mL) and heated at 50  $^\circ\text{C}$  for 30 min. After being cooled to rt., the solid was collected by filtration and dried in vacuo to give **7** (528.2 mg, 64.7 % yield), without further purification, proceed directly to the next step. Isopropylamine (756.7 mg, 10.1 mmol) was added to the solution of **7** (528.2 mg, 2.0 mmol) in MeCN (10 mL), the mixture was cooled to 15  $^\circ\text{C}$  and thereafter AcOH (362.4 mg, 6.04 mmol) was added under stirring. After stirring at 90  $^\circ\text{C}$  overnight, the reaction mixture was allowed to cool to the room temperature and concentrated under reduced pressure. The resulting residue was chromatographed over silica gel to give **8** (209.3 mg, 51.3 % yield) as white solid. FT-IR (KBr): 3345 (–NH), 3173 (–NH), 2973 (Ar-H), 1646 (–C=N)  $\text{cm}^{-1}$ ;  $^1\text{H}$  NMR (400 MHz,  $\text{DMSO}-d_6$ ):  $\delta$  8.78 (s, 1H), 7.51 (t,  $J$  = 8.0 Hz, 1H), 7.16 (d,  $J$  = 7.2 Hz, 1H), 6.52 (d,  $J$  = 8.0 Hz, 1H), 6.20 (s, 2H), 5.58–5.46 (m, 1H), 1.42 (d,  $J$  = 6.8 Hz, 6H);  $^{13}\text{C}$  NMR (101 MHz,  $\text{CDCl}_3$ ):  $\delta$  157.83, 151.50, 146.08, 141.71, 138.74, 114.60, 109.21, 48.42, 23.70; ESI-HRMS ( $m/z$ ) [ $M + H$ ] $^+$  calcd for  $\text{C}_{10}\text{H}_{13}\text{N}_5$ , 204.1171, found 204.1243.

***N*-(6-(4-isopropyl-4H-1, 2, 4-triazol-3-yl) pyridin-2-yl) isoquinoline-4-carboxamide (9a).** Isoquinoline-4-carboxylic acid (50 mg, 0.289 mmol) was added to the solution of **8** (70.2 mg, 0.346 mmol) in  $\text{CH}_2\text{Cl}_2$  (5 mL).

The mixture was cooled to 0  $^\circ\text{C}$  and thereafter  $\text{Et}_3\text{N}$  (204.4 mg, 2.02 mmol) and  $\text{T}_3\text{P}$  (688 mL, 2.310 mmol) were added under stirring. The reaction mixture was allowed to warm to the room temperature and was heated under reflux for 20 h. After completion, the reaction mixture was diluted with  $\text{CH}_2\text{Cl}_2$  (about 10 mL) and washed with a saturated aqueous solution of  $\text{NaHCO}_3$  ( $3 \times 20$  mL). The organic layer was dried over  $\text{Na}_2\text{SO}_4$  and the solvent was removed in vacuo. The residue separated by column chromatography silica gel to afford **9a** (10 mg, 25.8 %) as a white solid.  $^1\text{H}$  NMR (400 MHz,  $\text{DMSO}-d_6$ ):  $\delta$  11.26 (s, 1H), 9.46 (s, 1H), 8.83 (s, 1H), 8.78 (s, 1H), 8.30 (d,  $J$  = 8.4 Hz, 1H), 8.22 (t,  $J$  = 8.0 Hz, 2H), 8.03 (t,  $J$  = 8.0 Hz, 1H), 7.90 (dd,  $J$  = 7.6, 0.4 Hz, 1H), 7.89–7.84 (m, 1H), 7.78–7.71 (m, 1H), 5.78–5.61 (m, 1H), 1.36 (d,  $J$  = 6.8 Hz, 6H); ESI-HRMS ( $m/z$ ) [ $M + H$ ] $^+$  calcd for  $\text{C}_{20}\text{H}_{18}\text{N}_6\text{O}$ , 359.1542, found 359.1619.

***N*-(6-(4-isopropyl-4H-1, 2, 4-triazol-3-yl) quinolon-2-yl) quinolone-4-carboxamide (9b).** In a similar way to the preparation of **9a**, compound **9b** was obtained from quinoline-4-carboxylic acid as white solid, 52.3 % yield.  $^1\text{H}$  NMR (400 MHz,  $\text{CD}_3\text{OD}$ ):  $\delta$  9.05 (d,  $J$  = 4.4 Hz, 1H), 8.84 (s, 1H), 8.50 (d,  $J$  = 8.4 Hz, 1H), 8.30 (d,  $J$  = 8.4 Hz, 1H), 8.19 (d,  $J$  = 8.4 Hz, 1H), 8.13 (t,  $J$  = 8.0 Hz, 1H), 7.99 (d,  $J$  = 7.6 Hz, 1H), 7.91 (t,  $J$  = 7.6 Hz, 1H), 7.80 (d,  $J$  = 4.4 Hz, 1H), 7.76 (t,  $J$  = 7.6 Hz, 1H), 5.86–5.73 (m, 1H), 1.52 (d,  $J$  = 6.8 Hz, 6H); ESI-HRMS ( $m/z$ ) [ $M + \text{Na}$ ] $^+$  calcd for  $\text{C}_{20}\text{H}_{18}\text{N}_6\text{O}$ , 381.1542, found 381.1419.

***N*-(6-(4-isopropyl-4H-1, 2, 4-triazol-3-yl) pyridin-2-yl) isoquinoline-1-carboxamide (9c).** Isoquinoline-1-carboxylic acid (50 mg, 0.289 mmol), 1-ethyl-3-(3-dimethylaminopropyl) carbodiimide hydrochloride (EDCI, 55.4 mg, 0.289 mmol) and *N*-hydroxysuccinimide (NHS, 34.1 mg, 0.289 mmol) were added to the solution of **8** (59 mg, 0.346 mmol) in  $\text{CH}_2\text{Cl}_2$  (5 mL). After stirring for 7 h at 40  $^\circ\text{C}$ , the mixture was diluted with  $\text{CH}_2\text{Cl}_2$  (about 10 mL) and washed with a saturated aqueous solution of  $\text{NaHCO}_3$  ( $3 \times 20$  mL). The organic layer was dried over  $\text{Na}_2\text{SO}_4$  and the solvent was removed in vacuo. The residue separated by column chromatography silica gel to afford **9c** (24.5 mg, 23.7 %) as white solid.  $^1\text{H}$  NMR (400 MHz,  $\text{CDCl}_3$ ):  $\delta$  10.80 (s, 1H), 9.71–9.65 (m, 1H), 8.59 (t,  $J$  = 5.2 Hz, 2H), 8.06 (d,  $J$  = 5.2 Hz, 1H), 7.97 (d,  $J$  = 7.6 Hz, 1H), 7.94–7.90 (m, 2H), 7.82–7.73 (m, 2H), 5.88–5.68 (m, 1H), 1.63 (d,  $J$  = 2.4

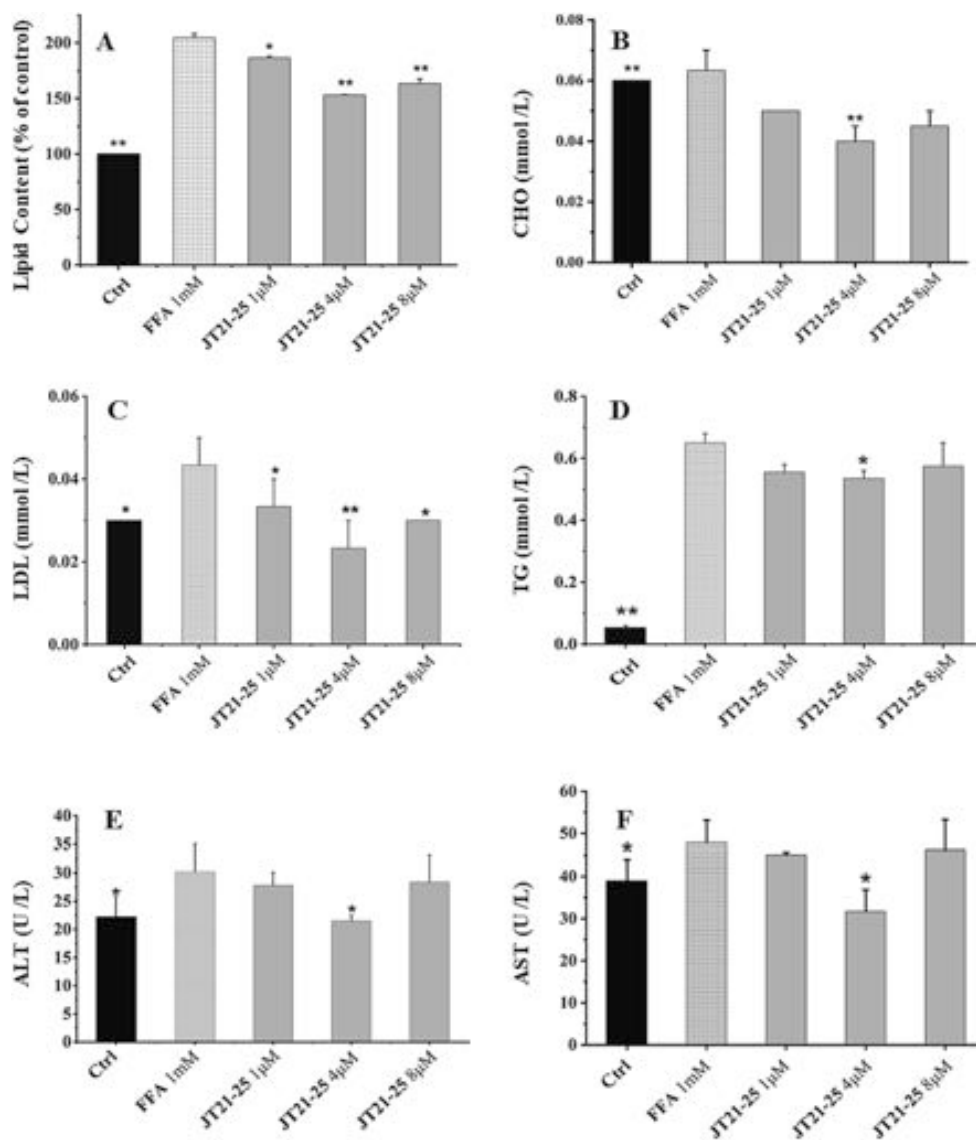


**Fig. 7.** The content of lipid droplets detected by a microplate reader at 492 nm in LO2 cells treated with different concentrations of JT21-25 (A); Effects of JT21-25 on CHOL (B), LDL (C), TG (D), ALT (E), AST (F) content in LO2 cells. \*  $p < 0.05$ , \*\* $p < 0.01$  vs. the FFA group.

**Table 5**

JT21-25 effects on AST, ALT in LO2 cells ( $\bar{x} \pm s$ ).

Groups	ALT <sup>a</sup> (U/L)	AST <sup>a</sup> (U/L)
Ctrl	22.26 $\pm$ 3.63*	38.931 $\pm$ 5.04*
FFA	30.22 $\pm$ 4.84	47.88 $\pm$ 5.25
JT21-25(1 $\mu$ M)	27.86 $\pm$ 2.21	45.05 $\pm$ 0.62
JT21-25(4 $\mu$ M)	21.49 $\pm$ 1.04*	31.69 $\pm$ 5.17*
JT21-25(8 $\mu$ M)	28.39 $\pm$ 4.82	46.17 $\pm$ 7.11

<sup>a</sup> Values are the means  $\pm$  SD from three independent experiments. \* $P < 0.05$ , \*\* $P < 0.01$  vs. the FFA group.

H<sub>z</sub>, 6H); ESI-HRMS ( $m/z$ ) [ $M + H$ ]<sup>+</sup> calcd for C<sub>20</sub>H<sub>18</sub>N<sub>6</sub>O, 359.1542, found 359.1622.

*N*-(6-(4-isopropyl-4H-1, 2, 4-triazol-3-yl) quinolon-2-yl) quinolone-2-carboxamide (**9d**). In a similar way to the preparation of **9c**, compound **9d** was obtained from quinoline-2-carboxylic acid as white solid, 26.6 % yield. <sup>1</sup>H NMR (400 MHz, CDCl<sub>3</sub>):  $\delta$  10.75 (s, 1H), 8.56 (d,  $J = 8.0$  Hz, 1H), 8.43 (s, 2H), 8.18 (d,  $J = 8.4$  Hz, 1H), 8.09 (d,  $J = 7.2$  Hz, 1H), 7.96 (d,  $J = 8.4$  Hz, 2H), 7.85 (t,  $J = 8.0$  Hz, 1H), 7.70 (t,  $J = 7.2$  Hz, 1H), 5.78 – 5.63 (m, 1H), 1.70 (d,  $J = 1.6$  Hz, 6H); ESI-HRMS ( $m/z$ ) [ $M + Na$ ]<sup>+</sup>

calcd for C<sub>20</sub>H<sub>18</sub>N<sub>6</sub>O, 381.1542, found 381.1433.

*5-bromo-N*-(6-(4-isopropyl-4H-1, 2, 4-triazol-3-yl) pyridin-2-yl) quinoline-2-carboxamide (**9e**). In a similar way to the preparation of **9a**, compound **9e** was obtained from 5-bromoquinoline-2-carboxylic acid as white solid, 64.3 % yield. <sup>1</sup>H NMR (400 MHz, CDCl<sub>3</sub>):  $\delta$  10.64 (s, 1H), 8.79 (d,  $J = 8.8$  Hz, 1H), 8.51 (dd,  $J = 11.2, 8.4$  Hz, 2H), 8.41 (s, 1H), 8.14 (d,  $J = 8.8$  Hz, 1H), 8.05 (d,  $J = 7.6$  Hz, 1H), 7.98 (d,  $J = 3.6$  Hz, 1H), 7.96 (d,  $J = 2.8$  Hz, 1H), 7.69 (t,  $J = 8.4$  Hz, 1H), 5.66 – 5.55 (m, 1H), 1.66 (d,  $J = 6.8$  Hz, 6H); ESI-HRMS ( $m/z$ ) [ $M + H$ ]<sup>+</sup> calcd for C<sub>20</sub>H<sub>17</sub>BrN<sub>6</sub>O, 437.0647, found 437.0710.

*6-bromo-N*-(6-(4-isopropyl-4H-1, 2, 4-triazol-3-yl) pyridin-2-yl) quinoline-2-carboxamide (**9f**). In a similar way to the preparation of **9a**, compound **9f** was obtained from 6-bromoquinoline-2-carboxylic acid as white solid, 55.5 % yield. <sup>1</sup>H NMR (400 MHz, CDCl<sub>3</sub>):  $\delta$  10.62 (s, 1H), 8.52 (d,  $J = 8.0$  Hz, 1H), 8.47 (s, 1H), 8.43 (d,  $J = 8.4$  Hz, 1H), 8.32 (d,  $J = 8.8$  Hz, 1H), 8.11 (s, 1H), 8.04 (dd,  $J = 7.6, 5.2$  Hz, 2H), 7.96 (t,  $J = 8.0$  Hz, 1H), 7.89 (dd,  $J = 8.8, 1.6$  Hz, 1H), 5.67 – 5.55 (m, 1H), 1.66 (d,  $J = 6.8$  Hz, 6H); ESI-HRMS ( $m/z$ ) [ $M + H$ ]<sup>+</sup> calcd for C<sub>20</sub>H<sub>17</sub>BrN<sub>6</sub>O, 437.0647, found 437.0733.

*N*-(6-(4-isopropyl-4H-1, 2, 4-triazol-3-yl) pyridin-2-yl)-5-(1-methyl-1, 2, 3, 6-tetrahydropyridin-4-yl) quinoline-2-carboxamide (**10a**). **9e** (141



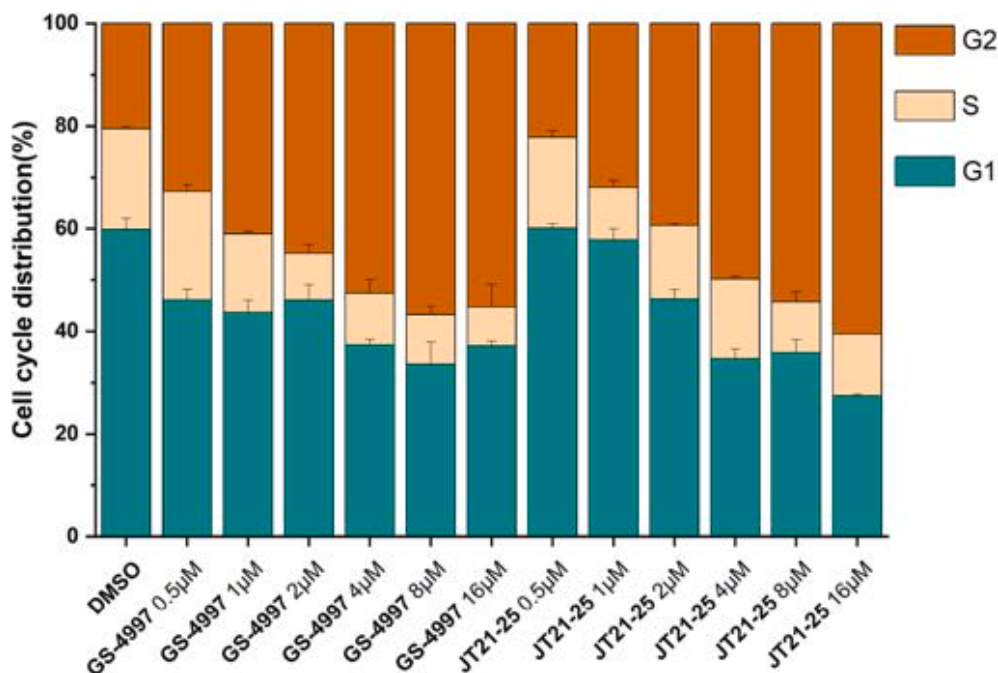


Fig. 8. Cell cycle distribution of HepG2 cells exposure to 0.5, 1, 2, 4, 8, and 16  $\mu$ M of JT21-25 and GS-4997 for 24 h.

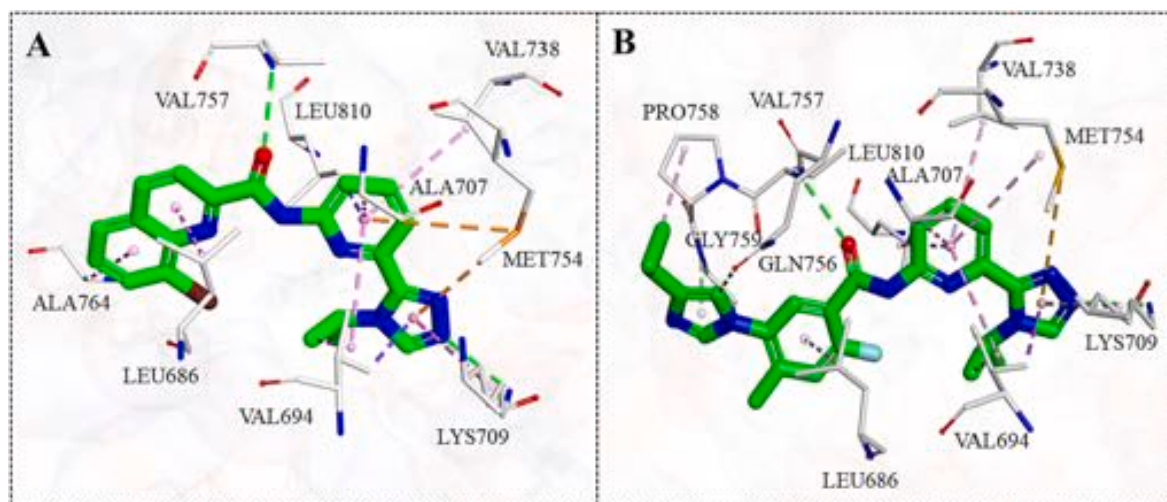


Fig. 9. Receptor-ligand interactions of JT21-25 (A) and GS-4997 (B) with ASK1 (PDB code: 5UOX).

mg, 1.0 mmol) was dissolved in DME/H<sub>2</sub>O (2 mL/2 mL), followed by addition of 1-methyl-4-(4, 4, 5, 5-tetramethyl-1,3,2-dioxaborolan-2-yl)-1, 2, 3, 6-tetrahydropyridine (22.5 mg, 0.1 mmol), sodium carbonate (48.5 mg, 0.45 mmol) and tetrakis(triphenylphosphine)palladium(0) (10.6 mg, 0.009 mmol). The mixture was stirred at 80 °C for 2 h, the reaction was monitored by TLC. Upon completion, the reaction mixture was cooled to rt. and the solvent was removed under reduced pressure. The residue separated by column chromatography silica gel to afford **10a** (20.6 mg, 50.5 %) as yellow solid. <sup>1</sup>H NMR (400 MHz, CDCl<sub>3</sub>):  $\delta$  10.71 (s, 1H), 8.64 (d,  $J$  = 8.8 Hz, 1H), 8.52 (dd,  $J$  = 8.4, 0.8 Hz, 1H), 8.40 (s, 1H), 8.36 (d,  $J$  = 8.8 Hz, 1H), 8.08 – 8.02 (m, 2H), 7.94 (t,  $J$  = 8.0 Hz, 1H), 7.76 (dd,  $J$  = 8.4, 7.2 Hz, 1H), 7.50 (dd,  $J$  = 7.2, 1.2 Hz, 1H), 5.82 – 5.78 (m, 1H), 5.68 – 5.57 (m, 1H), 3.27 (d,  $J$  = 2.8 Hz, 2H), 2.83 (t,  $J$  = 6.0 Hz, 2H), 2.63 (d,  $J$  = 2.0 Hz, 2H), 2.53 (s, 3H), 1.65 (d,  $J$  = 6.8 Hz, 6H); ESI-HRMS ( $m/z$ ) [ $M + H$ ]<sup>+</sup> calcd for C<sub>26</sub>H<sub>27</sub>N<sub>7</sub>O, 454.2277, found 454.2358.

*N*-(6-(4-isopropyl-4H-1, 2, 4-triazol-3-yl) pyridin-2-yl)-6-(1-methyl-1,

2, 3, 6-tetrahydropyridin-4-yl) quinoline-2-carboxamide (**10b**). In a similar way to the preparation of **10a**, compound **10b** was obtained from **9f** as yellow solid, 82.3 % yield. <sup>1</sup>H NMR (400 MHz, CDCl<sub>3</sub>):  $\delta$  10.69 (s, 1H), 8.52 (dd,  $J$  = 8.4, 0.8 Hz, 1H), 8.40 (s, 1H), 8.37 (s, 1H), 8.35 (s, 1H), 8.08 (d,  $J$  = 8.8 Hz, 1H), 8.03 (d,  $J$  = 6.8 Hz, 1H), 7.95 (t,  $J$  = 2.0, 1H), 7.94 – 7.91 (m, 1H), 7.82 (d,  $J$  = 1.6 Hz, 1H), 6.36 (t,  $J$  = 3.6, 1H), 5.68 – 5.56 (m, 1H), 3.24 (d,  $J$  = 3.2 Hz, 2H), 2.81 – 2.72 (m, 4H), 2.47 (s, 3H), 1.65 (d,  $J$  = 6.8 Hz, 6H); ESI-HRMS ( $m/z$ ) [ $M + H$ ]<sup>+</sup> calcd for C<sub>26</sub>H<sub>27</sub>N<sub>7</sub>O, 454.2277, found 454.2346.

7-bromo-*N*-(6-(4-isopropyl-4H-1, 2, 4-triazol-3-yl) pyridin-2-yl) quinoline-2-carboxamide (**9g**). In a similar way to the preparation of **9a**, compound **9g** was obtained from 7-bromoquinoline-2-carboxylic acid as white solid, 55.2 % yield. <sup>1</sup>H NMR (400 MHz, CDCl<sub>3</sub>):  $\delta$  10.58 (s, 1H), 8.52 (d,  $J$  = 8.4 Hz, 1H), 8.43 (d,  $J$  = 8.4 Hz, 2H), 8.39 (d,  $J$  = 8.4 Hz, 1H), 8.35 (d,  $J$  = 1.2 Hz, 1H), 8.06 (d,  $J$  = 7.6 Hz, 1H), 7.95 (t,  $J$  = 8.0 Hz, 1H), 7.82 (d,  $J$  = 8.8 Hz, 1H), 7.77 (dd,  $J$  = 8.8, 2.0 Hz, 1H), 5.68 – 5.55 (m, 1H), 1.67 (d,  $J$  = 6.8 Hz, 6H); ESI-HRMS ( $m/z$ ) [ $M + H$ ]<sup>+</sup> calcd

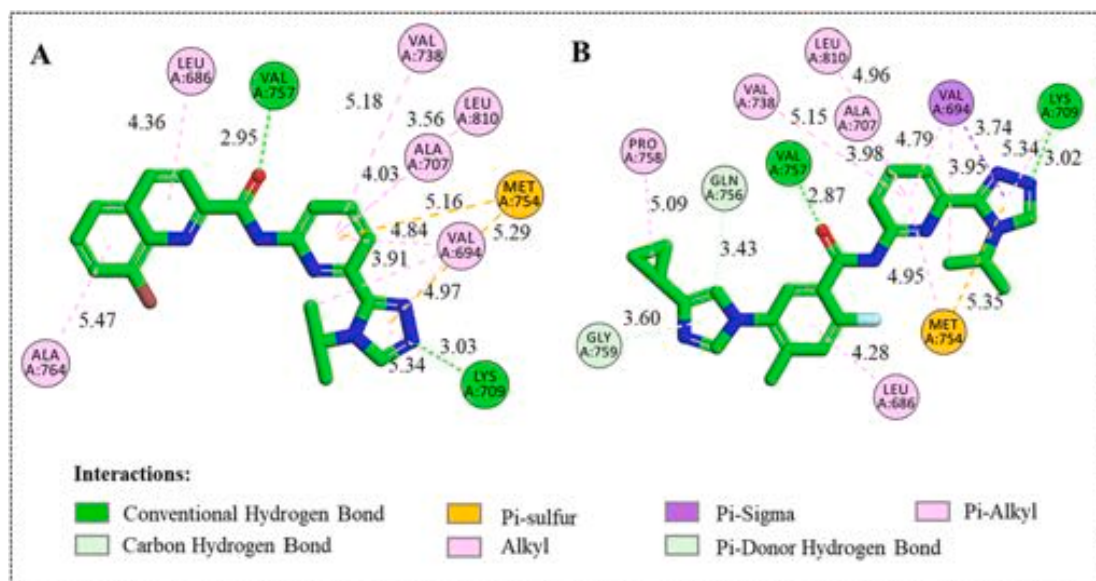


Fig. 10. Docking conformations of JT21-25 (A) and GS-4997 (B) with ASK1 (PDB code: 5UOX).

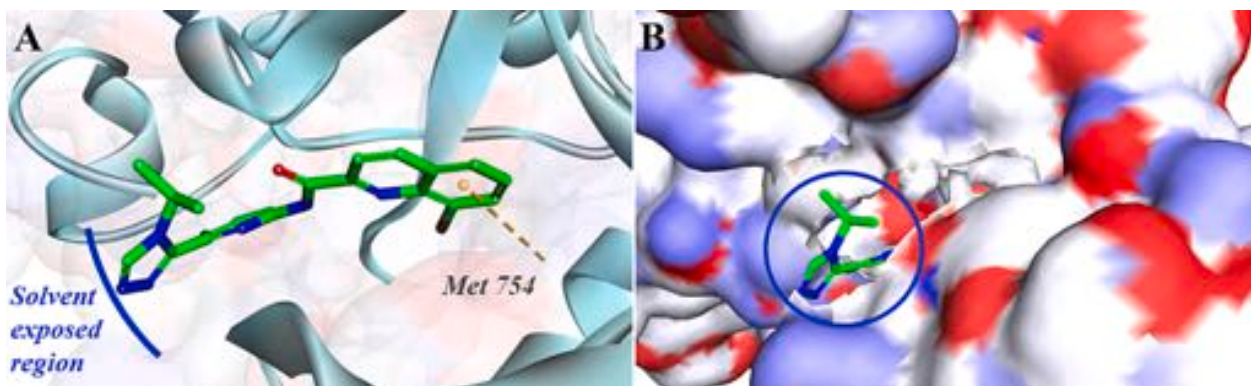


Fig. 11. Docking conformations of JT21-25 with TAK1 (PDB code: 2EVA).

Table 6

Calculated in silico ADME parameters of the synthesized JT21-25.

Compd.	MW <sup>a</sup> (≤500)	Physicochemical parameters					Bioavailability Score	PAINS alerts
		nrotb <sup>b</sup> (≤5)	nON <sup>c</sup> (≤10)	nOHNH <sup>d</sup> (≤5)	tPSA <sup>e</sup> (Å <sup>2</sup> )	iLOGP <sup>f</sup> (≤5)		
JT21-25	437.29	5	5	1	85.59	2.70	0.55	0

<sup>a</sup> MW: molecular weight.

<sup>b</sup> nrotb: number of rotatable bonds.

<sup>c</sup> nON: number of hydrogen acceptors.

<sup>d</sup> nOHNH: number of hydrogen donors.

<sup>e</sup> tPSA: total polar surface area.

<sup>f</sup> ilog P: octanol/water partition coefficient.

for C<sub>20</sub>H<sub>17</sub>BrN<sub>6</sub>O, 437.0647, found 437.0716.

*N*-(6-(4-isopropyl-4H-1, 2, 4-triazol-3-yl)pyridin-2-yl)-7-(1-methyl-1, 2, 3, 6-tetrahydropyridin-4-yl)quinoline-2-carboxamide (**10c**). In a similar way to the preparation of **10a**, compound **10c** was obtained from **9g** as yellow solid, 98.5 % yield. <sup>1</sup>H NMR (400 MHz, CDCl<sub>3</sub>): δ 10.68 (s, 1H), 8.52 (dd, *J* = 8.4, 0.8 Hz, 1H), 8.40 (s, 1H), 8.35 (s, 2H), 8.07 (d, *J* = 1.6 Hz, 1H), 8.01 (d, *J* = 6.8 Hz, 1H), 7.96 (d, *J* = 7.6 Hz, 1H), 7.87 (d, *J* = 8.8 Hz, 1H), 7.79 (dd, *J* = 8.8, 2.0 Hz, 1H), 6.35 (t, *J* = 3.6 Hz, 1H), 5.65 – 5.53 (m, 1H), 3.31 (d, *J* = 2.4 Hz, 2H), 2.86 (d, *J* = 4.4 Hz, 2H), 2.84 – 2.79 (m, 2H), 2.53 (s, 3H), 1.64 (d, *J* = 6.8 Hz, 6H); ESI-HRMS

(*m/z*) [*M* + *H*]<sup>+</sup> calcd for C<sub>26</sub>H<sub>27</sub>N<sub>7</sub>O, 454.2277, found 454.2357.

8-bromo-*N*-(6-(4-isopropyl-4H-1, 2, 4-triazol-3-yl)pyridin-2-yl)quinoline-2-carboxamide (**9h**). In a similar way to the preparation of **9a**, compound **9h** was obtained from 8-bromoquinoline-2-carboxylic acid as white solid, 40.9 % yield. <sup>1</sup>H NMR (400 MHz, CDCl<sub>3</sub>): δ 10.93 (s, 1H), 8.52 (d, *J* = 8.0 Hz, 1H), 8.49 – 8.41 (m, 2H), 8.41 (s, 1H), 8.16 (dd, *J* = 7.2, 0.8 Hz, 1H), 8.13 (d, *J* = 7.6 Hz, 1H), 7.98 – 7.90 (m, 2H), 7.55 (t, *J* = 7.6 Hz, 1H), 5.86 – 5.74 (m, 1H), 1.66 (d, *J* = 6.8 Hz, 6H); ESI-HRMS (*m/z*) [*M* + *H*]<sup>+</sup> calcd for C<sub>20</sub>H<sub>17</sub>BrN<sub>6</sub>O, 437.0647, found 437.0708.

*N*-(6-(4-isopropyl-4H-1, 2, 4-triazol-3-yl)pyridin-2-yl)-8-(1-methyl-



1, 2, 3, 6-tetrahydropyridin-4-yl) quinoline-2-carboxamide (**10d**). In a similar way to the preparation of **10a**, compound **10d** was obtained from **9h** as yellow solid, 99.5 % yield.  $^1\text{H}$  NMR (400 MHz,  $\text{CDCl}_3$ ):  $\delta$  10.45 (s, 1H), 8.49 (d,  $J$  = 8.0 Hz, 1H), 8.40 (s, 2H), 8.38 (s, 1H), 7.96 (t,  $J$  = 8.0 Hz, 1H), 7.86 (dd,  $J$  = 12.0, 8.0 Hz, 2H), 7.70 (d,  $J$  = 6.4 Hz, 1H), 7.62 (t,  $J$  = 7.6 Hz, 1H), 5.98 (s, 1H), 5.40 – 5.28 (m, 1H), 3.36 (s, 2H), 3.01 – 2.88 (m, 4H), 2.51 (s, 3H), 1.57 (d,  $J$  = 6.8 Hz, 6H); ESI-HRMS ( $m/z$ )  $[\text{M} + \text{H}]^+$  calcd for  $\text{C}_{26}\text{H}_{27}\text{N}_7\text{O}$ , 454.2277, found 454.2359.

3-(4-isopropyl-4H-1, 2, 4-triazol-3-yl) aniline (**14a**). To a solution of methyl 3-aminobenzoate (**11a**, 1.0 g, 6.6 mmol) in  $\text{CH}_3\text{OH}$  (15 mL) was added hydrazine hydrate (666.0 mg, 13.2 mmol), the mixture was stirred at 75 °C for 7 h, the reaction was monitored by TLC. Upon completion, the reaction mixture was concentrated under reduced pressure to give **12a** (1.0 g, 100 % yield) as a white solid. Without further purification, proceed directly to the next step. A mixture of **12a** (1.0 g, 6.6 mmol) in DMF-DMA was heated under reflux for 3 h, the reaction was monitored by TLC. Upon completion, the reaction mixture was cooled to rt. and then concentrated under reduced pressure. The residue was taken up in EA (100 mL) and heated at 50 °C for 30 min. After being cooled to rt., the solid was collected by filtration and dried in vacuo to give **13a** (916.9 mg, 53.2 % yield), without further purification, proceed directly to the next step. Isopropylamine (1035.8 mg, 17.6 mmol) was added to the solution of **13a** (916.9 mg, 3.5 mmol) in MeCN (15 mL), the mixture was cooled to 15 °C and thereafter AcOH (632 mg, 10.5 mmol) was added under stirring. After stirring at 90 °C overnight, the reaction mixture was allowed to cool to the room temperature and concentrated under reduced pressure. The resulting residue was chromatographed over silica gel to give **14a** (226.4 mg, 32 % yield) as white solid. FT-IR (KBr): 3443 (–NH), 3333 (–NH), 3092 (Ar-H), 1623 (C=N)  $\text{cm}^{-1}$ ;  $^1\text{H}$  NMR (400 MHz,  $\text{CDCl}_3$ ):  $\delta$  8.33 (s, 1H), 7.26 (t,  $J$  = 8.0 Hz, 1H), 6.92 (s, 1H), 6.86 (d,  $J$  = 7.6 Hz, 1H), 6.81 (dd,  $J$  = 8.0, 1.6 Hz, 1H), 4.60 – 4.48 (m, 1H), 1.47 (d,  $J$  = 6.4 Hz, 6H);  $^{13}\text{C}$  NMR (101 MHz,  $\text{DMSO}-d_6$ ):  $\delta$  153.09, 149.17, 141.86, 129.41, 128.03, 115.81, 115.08, 114.02, 47.24, 23.30; ESI-HRMS ( $m/z$ )  $[\text{M} + \text{H}]^+$  calcd for  $\text{C}_{11}\text{H}_{14}\text{N}_4$ , 203.1218, found 203.1296.

4-(4-isopropyl-4H-1, 2, 4-triazol-3-yl) pyridin-2-amine (**14b**). In a similar way to the preparation of **14a**, compound **14b** was obtained from methyl 2-aminoisonicotinate (**11b**) as yellow solid, 40 % yield. FT-IR (KBr): 3125 (–NH<sub>2</sub>), 1638 (C=N)  $\text{cm}^{-1}$ ;  $^1\text{H}$  NMR (400 MHz,  $\text{CDCl}_3$ ):  $\delta$  8.32 (s, 1H), 8.13 (d,  $J$  = 5.2 Hz, 1H), 6.79 (s, 1H), 6.69 (dd,  $J$  = 5.2, 1.2 Hz, 1H), 5.09 (s, 2H), 4.56 – 4.42 (m, 1H), 1.45 (d,  $J$  = 6.8 Hz, 6H);  $^{13}\text{C}$  NMR (101 MHz,  $\text{CDCl}_3$ ):  $\delta$  159.31, 151.96, 148.89, 141.52, 136.49, 112.58, 108.66, 48.08, 23.96; ESI-HRMS ( $m/z$ )  $[\text{M} + \text{H}]^+$  calcd for  $\text{C}_{10}\text{H}_{13}\text{N}_5$ , 204.1171, found 204.1249.

5-(4-isopropyl-4H-1, 2, 4-triazol-3-yl) pyridin-3-amine (**14c**). In a similar way to the preparation of **14a**, compound **14c** was obtained from methyl 5-aminonicotinate (**11c**) as yellow oil, 39.5 % yield. FT-IR (KBr): 3351 (–NH), 3190 (–NH), 1647 (C=N)  $\text{cm}^{-1}$ ;  $^1\text{H}$  NMR (400 MHz,  $\text{DMSO}-d_6$ ):  $\delta$  8.87 (s, 1H), 8.07 (d,  $J$  = 2.8 Hz, 1H), 7.91 – 7.87 (m, 1H), 7.10 (t,  $J$  = 2.0 Hz, 1H), 4.45 – 4.32 (m, 1H), 1.41 (d,  $J$  = 6.8 Hz, 6H);  $^{13}\text{C}$  NMR (101 MHz,  $\text{DMSO}-d_6$ ):  $\delta$  150.74, 144.86, 142.43, 137.44, 135.98, 123.66, 119.35, 47.56, 23.31; ESI-HRMS ( $m/z$ )  $[\text{M} + \text{H}]^+$  calcd for  $\text{C}_{10}\text{H}_{13}\text{N}_5$ , 204.1171, found 204.1251.

2-(4-isopropyl-4H-1, 2, 4-triazol-3-yl) pyridin-4-amine (**14d**). In a similar way to the preparation of **14a**, compound **14d** was obtained from methyl 4-aminopicolinate (**11d**) as yellow solid, 39.1 % yield. FT-IR (KBr): 3381 (–NH), 3196 (–NH), 1659 (C=N)  $\text{cm}^{-1}$ ;  $^1\text{H}$  NMR (400 MHz,  $\text{CDCl}_3$ ):  $\delta$  8.28 (s, 1H), 8.15 (d,  $J$  = 5.6 Hz, 1H), 7.50 (d,  $J$  = 2.4 Hz, 1H), 6.53 (dd,  $J$  = 5.6, 2.4 Hz, 1H), 4.75 – 4.63 (m, 1H), 1.44 (d,  $J$  = 6.8 Hz, 6H);  $^{13}\text{C}$  NMR (101 MHz,  $\text{CDCl}_3$ ):  $\delta$  153.97, 151.78, 149.45, 148.30, 141.78, 141.13, 109.70, 48.49, 48.40, 23.64; ESI-HRMS ( $m/z$ )  $[\text{M} + \text{H}]^+$  calcd for  $\text{C}_{10}\text{H}_{13}\text{N}_5$ , 204.1171, found 204.1255.

6-(4-isopropyl-4H-1, 2, 4-triazol-3-yl)pyrazin-2-amine (**14e**). In a similar way to the preparation of **14a**, compound **14e** was obtained from methyl 6-aminopyrazine-2-carboxylate (**11e**) as yellow solid, 56.5 % yield. FT-IR (KBr): 3318 (–NH), 3158 (–NH), 1644 (C=N)  $\text{cm}^{-1}$ ;  $^1\text{H}$

NMR (400 MHz,  $\text{CDCl}_3$ ):  $\delta$  8.78 (s, 1H), 8.38 (s, 1H), 8.05 (s, 1H), 5.52 – 5.39 (m, 1H), 1.53 (d,  $J$  = 6.8 Hz, 6H);  $^{13}\text{C}$  NMR (101 MHz,  $\text{CDCl}_3$ ):  $\delta$  153.35, 149.50, 142.15, 140.70, 134.02, 132.61, 48.67, 23.73; ESI-HRMS ( $m/z$ )  $[\text{M} + \text{H}]^+$  calcd for  $\text{C}_9\text{H}_{12}\text{N}_6$ , 205.1123, found 205.1186.

N-(3-(4-isopropyl-4H-1, 2, 4-triazol-3-yl) phenyl) quinoline-2-carboxamide (**15a**). Quinoline-2-carboxylic acid (40 mg, 0.23 mmol) was added to the solution of **14a** (46.7 mg, 0.15 mmol) in pyridine (3 mL). The reaction was in an argon environment, and then slowly added  $\text{POCl}_3$  (141.8 mg, 0.92 mmol), the mixture was stirred at rt. for 3 h. Upon completion, the mixture was acidified with 2 M hydrochloric acid solution until the precipitated formed was separated. The precipitate formed was filtered off, washed once with water, evaporated to dryness and then separated by column chromatography silica gel to afford **15a** (39.2 mg, 47.7 %) as white solid.  $^1\text{H}$  NMR (400 MHz,  $\text{CDCl}_3$ ):  $\delta$  10.42 (s, 1H), 8.38 (s, 1H), 8.37 (s, 2H), 8.18 (d,  $J$  = 12.4 Hz, 2H), 7.98 (d,  $J$  = 8.8 Hz, 1H), 7.91 (d,  $J$  = 8.0 Hz, 1H), 7.82 (t,  $J$  = 7.2 Hz, 1H), 7.66 (t,  $J$  = 7.2 Hz, 1H), 7.56 (t,  $J$  = 7.6 Hz, 1H), 7.41 (d,  $J$  = 7.6 Hz, 1H), 4.72 – 4.59 (m, 1H), 1.55 (d,  $J$  = 6.8 Hz, 6H); ESI-HRMS ( $m/z$ )  $[\text{M} + \text{H}]^+$  calcd for  $\text{C}_{21}\text{H}_{19}\text{N}_5\text{O}$ , 358.1590, found 358.1668.

N-(4-(4-isopropyl-4H-1, 2, 4-triazol-3-yl) pyridin-2-yl) quinoline-2-carboxamide (**15b**). In a similar way to the preparation of **15a**, compound **15b** was obtained from **14b** as white solid, 38.8 % yield.  $^1\text{H}$  NMR (400 MHz,  $\text{CDCl}_3$ ):  $\delta$  10.97 (s, 1H), 8.76 (s, 1H), 8.58 (d,  $J$  = 5.2 Hz, 1H), 8.46 (s, 1H), 8.40 (d,  $J$  = 8.8 Hz, 1H), 8.36 (d,  $J$  = 8.8 Hz, 1H), 8.23 (d,  $J$  = 8.4 Hz, 1H), 7.93 (d,  $J$  = 8.0 Hz, 1H), 7.83 (t,  $J$  = 7.2 Hz, 1H), 7.68 (t,  $J$  = 7.2 Hz, 1H), 7.55 (d,  $J$  = 4.0 Hz, 1H), 4.83 – 4.70 (m, 1H), 1.63 (d,  $J$  = 6.4 Hz, 6H). ESI-HRMS ( $m/z$ )  $[\text{M} + \text{H}]^+$  calcd for  $\text{C}_{20}\text{H}_{18}\text{N}_6\text{O}$ , 359.1542, found 359.1620.

N-(4-(4-isopropyl-4H-1, 2, 4-triazol-3-yl) pyridin-2-yl) quinoline-2-carboxamide (**15c**). In a similar way to the preparation of **15a**, compound **15c** was obtained from **14c** as white solid, 30.7 % yield.  $^1\text{H}$  NMR (400 MHz,  $\text{CDCl}_3$ ):  $\delta$  10.53 (s, 1H), 9.10 (s, 1H), 8.81 (s, 1H), 8.70 (s, 1H), 8.48 (s, 1H), 8.40 (dd,  $J$  = 18.0, 8.4 Hz, 2H), 8.22 (d,  $J$  = 8.4 Hz, 1H), 7.95 (d,  $J$  = 8.0 Hz, 1H), 7.86 (t,  $J$  = 7.4 Hz, 1H), 7.70 (t,  $J$  = 7.4 Hz, 1H), 4.71 – 4.53 (m, 1H), 1.60 (d,  $J$  = 6.4 Hz, 6H); ESI-HRMS ( $m/z$ )  $[\text{M} + \text{H}]^+$  calcd for  $\text{C}_{20}\text{H}_{18}\text{N}_6\text{O}$ , 359.1542, found 359.1635.

N-(2-(4-isopropyl-4H-1, 2, 4-triazol-3-yl) pyridin-4-yl) quinoline-2-carboxamide (**15d**). In a similar way to the preparation of **15a**, compound **15d** was obtained from **14d** as white solid, 43.5 % yield.  $^1\text{H}$  NMR (400 MHz,  $\text{CDCl}_3$ ):  $\delta$  10.63 (s, 1H), 8.64 (d,  $J$  = 5.6 Hz, 1H), 8.44 – 8.37 (m, 4H), 8.31 (d,  $J$  = 2.0 Hz, 1H), 8.20 (d,  $J$  = 8.4 Hz, 1H), 7.93 (d,  $J$  = 8.0 Hz, 1H), 7.90 – 7.82 (m, 1H), 7.72 – 7.66 (m, 1H), 5.91 – 5.79 (m, 1H), 1.56 (d,  $J$  = 6.8 Hz, 6H); ESI-HRMS ( $m/z$ )  $[\text{M} + \text{H}]^+$  calcd for  $\text{C}_{20}\text{H}_{18}\text{N}_6\text{O}$ , 359.1542, found 359.1625.

N-(6-(4-isopropyl-4H-1, 2, 4-triazol-3-yl) pyrazin-2-yl)quinoline-2-carboxamide (**15e**). In a similar way to the preparation of **15a**, compound **15e** was obtained from **14e** as white solid, 57.9 % yield.  $^1\text{H}$  NMR (400 MHz,  $\text{CDCl}_3$ ):  $\delta$  10.72 (s, 1H), 9.85 (s, 1H), 9.31 (s, 1H), 8.47 (s, 1H), 8.43 (d,  $J$  = 2.4 Hz, 2H), 8.19 (d,  $J$  = 8.4 Hz, 1H), 7.97 (d,  $J$  = 8.0 Hz, 1H), 7.89 – 7.82 (m, 1H), 7.75 – 7.68 (m, 1H), 5.57 – 5.46 (m, 1H), 1.66 (d,  $J$  = 6.8 Hz, 6H); ESI-HRMS ( $m/z$ )  $[\text{M} + \text{Na}]^+$  calcd for  $\text{C}_{19}\text{H}_{17}\text{N}_7\text{O}$ , 382.1495, found 382.1396.

6-(1-isopropyl-1H-pyrazol-5-yl) pyridin-2-amine (**17a**). A mixture of 6-bromopyridin-2-amine (**16**, 100 mg, 0.58 mmol), 1-isopropyl-5-(4,4,5,5-tetramethyl-1,3,2-dioxaborolan-2-yl)-1H-pyrazole (273 mg, 1.16 mmol), Xphos-Pd-G2 (45.4 mg, 0.058 mmol) and  $\text{Na}_2\text{CO}_3$  (612.68 mg, 5.78 mmol) in dioxane/ $\text{H}_2\text{O}$  (5 mL/1 mL) was heated for 2 h at 100 °C under an argon atmosphere. Upon completion, the resulting mixture was dissolved in water and extracted with  $\text{CH}_2\text{Cl}_2$  (30 mL  $\times$  3). The combined organic layers were dried over anhydrous  $\text{Na}_2\text{SO}_4$ , filtered, and concentrated under reduced pressure. The resulting residue was chromatographed over silica gel to afford **17a** (60 mg, 51.3 % yield) as slightly yellow solid. FT-IR (KBr): 3369 (–NH), 3178 (–NH), 1635 (C=N)  $\text{cm}^{-1}$ ;  $^1\text{H}$  NMR (400 MHz,  $\text{CDCl}_3$ ):  $\delta$  7.53 (d,  $J$  = 1.6 Hz, 1H), 7.50 (dd,  $J$  = 8.4, 7.6 Hz, 1H), 6.87 (dd,  $J$  = 7.2, 0.8 Hz, 1H), 6.48 (dd,  $J$  = 8.4, 0.8 Hz, 1H), 6.43 (d,  $J$  = 2.0 Hz, 1H), 5.38 – 5.26 (m, 1H), 4.59 (s,

2H), 1.50 (d,  $J = 6.4$  Hz, 6H);  $^{13}\text{C}$  NMR (101 MHz,  $\text{CDCl}_3$ ):  $\delta$  157.99, 148.66, 141.03, 138.48, 138.18, 113.91, 107.56, 106.26, 50.79, 22.89; ESI-HRMS ( $m/z$ ) [ $M + H$ ] $^+$  calcd for  $\text{C}_{11}\text{H}_{14}\text{N}_4$ , 203.1218, found 203.1297.

(S)-2-(3-(6-aminopyridin-2-yl)-4H-1, 2, 4-triazol-4-yl) propan-1-ol (**17b**). In a similar way to the preparation of **8**, compound **17b** was obtained from **6** and (R)-2-aminopropan-1-ol instead of isopropylamine as lightly yellow solid, 79.5 % yield. FT-IR (KBr): 3217 (–NH), 3140 (–NH), 2866 (–OH), 1644 (–C=N)  $\text{cm}^{-1}$ ;  $^1\text{H}$  NMR (400 MHz,  $\text{DMSO}-d_6$ ):  $\delta$  8.68 (s, 1H), 7.51 (t,  $J = 8.0$  Hz, 1H), 7.17 (d,  $J = 7.2$  Hz, 1H), 6.51 (d,  $J = 8.0$  Hz, 1H), 6.17 (s, 2H), 5.47 – 5.35 (m, 1H), 3.65 – 3.59 (m, 2H), 1.42 (d,  $J = 6.8$  Hz, 3H);  $^{13}\text{C}$  NMR (101 MHz,  $\text{DMSO}-d_6$ ):  $\delta$  159.17, 151.33, 145.84, 143.32, 138.17, 111.68, 108.56, 64.37, 45.29, 17.71; ESI-HRMS ( $m/z$ ) [ $M + H$ ] $^+$  calcd for  $\text{C}_{10}\text{H}_{13}\text{N}_5\text{O}$ , 220.1120, found 220.1195.

(R)-2-(3-(6-aminopyridin-2-yl)-4H-1, 2, 4-triazol-4-yl) propan-1-ol (**17c**). In a similar way to the preparation of **8**, compound **17c** was obtained from **6** and (S)-2-aminopropan-1-ol instead of isopropylamine as lightly yellow solid, 26.4 % yield. FT-IR (KBr): 3330 (–NH), 3223 (–NH), 3134 (–OH), 1650 (–C=N)  $\text{cm}^{-1}$ ;  $^1\text{H}$  NMR (400 MHz,  $\text{DMSO}-d_6$ ):  $\delta$  8.68 (s, 1H), 7.51 (t,  $J = 7.8$  Hz, 1H), 7.17 (d,  $J = 7.2$  Hz, 1H), 6.51 (dd,  $J = 8.4$ , 0.8 Hz, 1H), 6.16 (d,  $J = 5.2$  Hz, 1H), 5.46 – 5.36 (m, 1H), 3.65 (dd,  $J = 11.2$ , 6.4 Hz, 1H), 3.59 (dd,  $J = 11.2$ , 4.8 Hz, 1H), 1.42 (d,  $J = 6.8$  Hz, 3H);  $^{13}\text{C}$  NMR (101 MHz,  $\text{DMSO}-d_6$ ):  $\delta$  159.12, 151.31, 145.89, 143.29, 138.12, 111.63, 108.48, 64.39, 53.28, 17.71; ESI-HRMS ( $m/z$ ) [ $M + H$ ] $^+$  calcd for  $\text{C}_{10}\text{H}_{13}\text{N}_5\text{O}$ , 220.1120, found 220.1183.

6-(4-cyclopropyl-4H-1, 2, 4-triazol-3-yl) pyridin-2-amine (**17d**). In a similar way to the preparation of **8**, compound **17d** was obtained from **6** and cyclopropanamine instead of isopropylamine as white solid, 50.7 % yield. FT-IR (KBr): 3312 (–NH), 3187 (–NH), 2914 (Ar-H), 1647 (–C=N)  $\text{cm}^{-1}$ ;  $^1\text{H}$  NMR (400 MHz,  $\text{CDCl}_3$ ):  $\delta$  8.14 (s, 1H), 7.53 (t,  $J = 8.0$  Hz, 1H), 7.46 (d,  $J = 7.2$  Hz, 1H), 6.58 (d,  $J = 8.0$  Hz, 1H), 3.91 – 3.81 (m, 1H), 1.05 (dd,  $J = 13.4$ , 6.4 Hz, 2H), 0.89 – 0.82 (m, 2H);  $^{13}\text{C}$  NMR (101 MHz,  $\text{DMSO}-d_6$ ):  $\delta$  163.43, 158.62, 147.84, 143.63, 138.10, 111.22, 109.80, 25.86, 6.05; ESI-HRMS ( $m/z$ ) [ $M + H$ ] $^+$  calcd for  $\text{C}_{10}\text{H}_{11}\text{N}_5$ , 202.1014, found 202.1092.

6-(4-cyclobutyl-4H-1, 2, 4-triazol-3-yl) pyridin-2-amine (**17e**). In a similar way to the preparation of **8**, compound **17e** was obtained from **6** and cyclobutanamine instead of isopropylamine as yellow solid, 65.1 % yield. FT-IR (KBr): 3470 (–NH), 3303 (–NH), 2973 (Ar-H), 1659 (–C=N)  $\text{cm}^{-1}$ ;  $^1\text{H}$  NMR (400 MHz,  $\text{CDCl}_3$ ):  $\delta$  8.36 (s, 1H), 7.57 – 7.52 (m, 1H), 7.49 (dd,  $J = 7.6$ , 0.8 Hz, 1H), 6.58 (dd,  $J = 7.6$ , 0.8 Hz, 1H), 5.53 – 5.41 (m, 1H), 2.60 – 2.51 (m, 2H), 2.32 – 2.28 (m, 2H), 1.88 – 1.78 (m, 2H);  $^{13}\text{C}$  NMR (101 MHz,  $\text{DMSO}-d_6$ ):  $\delta$  159.18, 151.04, 145.34, 143.62, 138.06, 111.19, 108.53, 49.64, 30.79, 14.34; ESI-HRMS ( $m/z$ ) [ $M + H$ ] $^+$  calcd for  $\text{C}_{11}\text{H}_{13}\text{N}_5$ , 216.1171, found 216.1249.

6-(4-cyclopentyl-4H-1, 2, 4-triazol-3-yl) pyridin-2-amine (**17f**). In a similar way to the preparation of **8**, compound **17f** was obtained from **6** and cyclopentanamine instead of isopropylamine as white solid, 17.6 % yield. FT-IR (KBr): 3419 (–NH), 3300 (–NH), 3190 (Ar-H), 1620 (–C=N)  $\text{cm}^{-1}$ ;  $^1\text{H}$  NMR (400 MHz,  $\text{CDCl}_3$ ):  $\delta$  8.28 (s, 1H), 7.59 – 7.50 (m, 2H), 6.58 (dd,  $J = 8.0$ , 1.2 Hz, 1H), 5.63 – 5.50 (m, 1H), 2.30 – 2.18 (m, 2H), 1.92 – 1.69 (m, 6H);  $^{13}\text{C}$  NMR (101 MHz,  $\text{CDCl}_3$ ):  $\delta$  157.70, 152.11, 145.85, 142.26, 138.86, 114.79, 109.37, 57.62, 33.98, 24.03. ESI-HRMS ( $m/z$ ) [ $M + H$ ] $^+$  calcd for  $\text{C}_{12}\text{H}_{15}\text{N}_5$ , 230.1327, found 230.1405.

N-(6-(1-isopropyl-1H-pyrazol-5-yl)pyridin-2-yl)quinoline-2-carboxamide (**18a**). In a similar way to the preparation of **15a**, compound **18a** was obtained from **17a** as white solid, 75.6 % yield.  $^1\text{H}$  NMR (400 MHz,  $\text{CDCl}_3$ ):  $\delta$  10.80 (s, 1H), 8.46 (dd,  $J = 8.4$ , 0.8 Hz, 1H), 8.41 (s, 2H), 8.19 (d,  $J = 8.8$  Hz, 1H), 7.93 (dd,  $J = 8.4$ , 0.8 Hz, 1H), 7.90 – 7.81 (m, 2H), 7.72 – 7.65 (m, 1H), 7.60 (d,  $J = 2.0$  Hz, 1H), 7.34 (dd,  $J = 7.6$ , 0.8 Hz, 1H), 6.54 (d,  $J = 2.0$  Hz, 1H), 5.36 (m, 1H), 1.61 (d,  $J = 6.8$  Hz, 6H); ESI-HRMS ( $m/z$ ) [ $M + H$ ] $^+$  calcd for  $\text{C}_{21}\text{H}_{19}\text{N}_5\text{O}$ , 358.1590, found 358.1699.

(S)-N-(6-(4-(1-hydroxypropan-2-yl)-4H-1, 2, 4-triazol-3-yl) pyridin-2-yl) quinoline-2-carboxamide (**18b**). Thionyl chloride ( $\text{SOCl}_2$ , 65 mg, 0.55 mmol) was slowly added to the stirred solution of quinoline-2-

carboxylic acid (70.9 mg, 0.41 mmol) in anhydrous toluene (4 mL). The mixture was stirred at  $80^\circ\text{C}$  for 2 h, the reaction was monitored by TLC. Upon completion, the reaction solution was concentrated under reduced pressure to dryness. The dry residue was dissolved in anhydrous toluene (4 mL) and added **17b** (50 mg, 0.23 mmol) and DIPEA (59 mg, 0.46 mmol). After the mixture was stirred at  $80^\circ\text{C}$  for 2 h, the solvent was evaporated to dryness. The dry residue was dissolved in  $\text{CH}_2\text{Cl}_2$  (20 mL) and washed with a saturated aqueous solution of  $\text{NaHCO}_3$  ( $3 \times 20$  mL). The organic layer was dried over  $\text{Na}_2\text{SO}_4$  and the solvent was removed in vacuo. The residue separated by column chromatography silica gel to afford **18b** (23 mg, 26.7 %) as white solid.  $^1\text{H}$  NMR (400 MHz,  $\text{DMSO}-d_6$ ):  $\delta$  10.78 (s, 1H), 8.80 (s, 1H), 8.64 (d,  $J = 8.4$  Hz, 1H), 8.31 (d,  $J = 8.4$  Hz, 1H), 8.25 (d,  $J = 8.8$  Hz, 1H), 8.18 (d,  $J = 8.4$  Hz, 1H), 8.10 (d,  $J = 8.0$  Hz, 1H), 8.06 (t,  $J = 8.0$  Hz, 1H), 7.93 – 7.82 (m, 2H), 7.74 (t,  $J = 8.0$  Hz, 1H), 5.44 – 5.33 (m, 1H), 3.74 – 3.65 (m, 2H), 1.50 (d,  $J = 7.2$  Hz, 3H); ESI-HRMS ( $m/z$ ) [ $M + H$ ] $^+$  calcd for  $\text{C}_{20}\text{H}_{18}\text{N}_6\text{O}_2$ , 375.1491, found 375.1569.

(R)-N-(6-(4-(1-hydroxypropan-2-yl)-4H-1, 2, 4-triazol-3-yl) pyridin-2-yl) quinoline-2-carboxamide (**18c**). In a similar way to the preparation of **9c**, compound **18c** was obtained from **17b** as white solid, 31.3 % yield.  $^1\text{H}$  NMR (400 MHz,  $\text{DMSO}-d_6$ ):  $\delta$  8.94 (s, 1H), 8.47 (d,  $J = 8.4$  Hz, 1H), 8.08 (d,  $J = 8.4$  Hz, 1H), 8.04 (d,  $J = 7.6$  Hz, 1H), 7.87 – 7.80 (m, 2H), 7.75 – 7.68 (m, 1H), 7.37 (dd,  $J = 8.4$ , 7.6 Hz, 1H), 7.10 (d,  $J = 7.6$  Hz, 1H), 6.42 (d,  $J = 7.6$  Hz, 1H), 6.16 (s, 2H), 6.06 – 5.96 (m, 1H), 4.74 – 4.58 (m, 2H), 1.60 (d,  $J = 7.2$  Hz, 3H); ESI-HRMS ( $m/z$ ) [ $M + H$ ] $^+$  calcd for  $\text{C}_{20}\text{H}_{18}\text{N}_6\text{O}_2$ , 375.1491, found 375.1570.

N-(6-(4-cyclopropyl-4H-1, 2, 4-triazol-3-yl) pyridin-2-yl) quinoline-2-carboxamide (**18d**). In a similar way to the preparation of **15a**, compound **18d** was obtained from **17d** as white solid, 76.3 % yield.  $^1\text{H}$  NMR (400 MHz,  $\text{CDCl}_3$ ):  $\delta$  10.75 (s, 1H), 8.55 (dd,  $J = 8.0$ , 0.8 Hz, 1H), 8.41 (s, 2H), 8.31 (s, 1H), 8.17 (d,  $J = 8.4$  Hz, 1H), 7.99 (dd,  $J = 7.6$ , 0.8 Hz, 1H), 7.95 (t,  $J = 8.0$  Hz, 2H), 7.87 – 7.79 (m, 1H), 7.72 – 7.64 (m, 1H), 4.02 – 3.92 (m, 1H), 1.28 – 1.20 (m, 2H), 1.06 – 0.98 (m, 2H); ESI-HRMS ( $m/z$ ) [ $M + H$ ] $^+$  calcd for  $\text{C}_{20}\text{H}_{16}\text{N}_6\text{O}$ , 357.1386, found 357.1464.

N-(6-(4-cyclobutyl-4H-1, 2, 4-triazol-3-yl) pyridin-2-yl) quinoline-2-carboxamide (**18e**). In a similar way to the preparation of **15a**, compound **18e** was obtained from **17e** as white solid, 74.9 % yield.  $^1\text{H}$  NMR (400 MHz,  $\text{CDCl}_3$ ):  $\delta$  10.40 (s, 1H), 9.80 (s, 1H), 8.51 (d,  $J = 8.0$  Hz, 2H), 8.28 – 8.23 (m, 1H), 8.21 – 8.16 (m, 1H), 8.04 (d,  $J = 7.2$  Hz, 1H), 7.99 – 7.89 (m, 3H), 5.59 – 5.47 (m, 1H), 2.76 – 2.64 (m, 2H), 2.48 – 2.37 (m, 2H), 2.05 – 1.98 (m, 2H); ESI-HRMS ( $m/z$ ) [ $M + H$ ] $^+$  calcd for  $\text{C}_{21}\text{H}_{18}\text{N}_6\text{O}$ , 371.1542, found 371.1620.

N-(6-(4-cyclopentyl-4H-1, 2, 4-triazol-3-yl) pyridin-2-yl) quinoline-2-carboxamide (**18f**). In a similar way to the preparation of **15a**, compound **18f** was obtained from **17f** as white solid, 96.4 % yield.  $^1\text{H}$  NMR (400 MHz,  $\text{CDCl}_3$ ):  $\delta$  10.75 (s, 1H), 8.52 (dd,  $J = 8.4$ , 0.8 Hz, 1H), 8.43 (s, 1H), 8.41 (s, 1H), 8.13 (d,  $J = 8.4$  Hz, 1H), 8.04 (dd,  $J = 7.6$ , 0.8 Hz, 1H), 7.99 – 7.92 (m, 2H), 7.88 – 7.80 (m, 1H), 7.72 – 7.65 (m, 1H), 5.71 – 5.58 (m, 1H), 2.46 – 2.37 (m, 2H), 2.02 – 1.88 (m, 6H); ESI-HRMS ( $m/z$ ) [ $M + H$ ] $^+$  calcd for  $\text{C}_{22}\text{H}_{20}\text{N}_6\text{O}$ , 385.1699, found 385.1777.

(S)-8-bromo-N-(6-(4-(1-hydroxypropan-2-yl)-4H-1, 2, 4-triazol-3-yl) pyridin-2-yl) quinoline-2-carboxamide (**19**). In a similar way to the preparation of **18b**, compound **19** was obtained from **17b** and 8-bromoquinoline-2-carboxylic acid as white solid, 19.0 % yield.  $^1\text{H}$  NMR (400 MHz,  $\text{CD}_3\text{OD}$ ):  $\delta$  9.63 (s, 1H), 8.65 (t,  $J = 8.4$  Hz, 2H), 8.44 (d,  $J = 8.4$  Hz, 1H), 8.26 (dd,  $J = 7.6$ , 1.2 Hz, 1H), 8.16 (t,  $J = 8.0$  Hz, 1H), 8.09 (dd,  $J = 8.4$ , 1.2 Hz, 1H), 8.00 (d,  $J = 7.2$  Hz, 1H), 7.67 – 7.63 (m, 1H), 5.88 – 5.77 (m, 1H), 4.09 (dd,  $J = 12.0$ , 3.6 Hz, 1H), 3.96 (dd,  $J = 12.0$ , 5.6 Hz, 1H), 1.74 (d,  $J = 7.2$  Hz, 3H); ESI-HRMS ( $m/z$ ) [ $M + H$ ] $^+$  calcd for  $\text{C}_{20}\text{H}_{17}\text{BrN}_6\text{O}_2$ , 453.0596, found 453.0674.

#### 4.3. ASK1 kinase inhibition assay

A multifunctional enzyme marker (2104 Multilabel Reader, Perkin Elmer, USA) is used to detect ASK1 inhibitory activity. The biochemical incubator is sourced from Biochemical Incubator, while the ultrasonic

nanoliter liquid treatment system is purchased from Echo. ASK1 inhibitory activity was evaluated by ADP-Glo Luminescent Assay. ASK1 kinase (Eurofins, Belgium) and the substrate were diluted with HTRF kinase buffer solution (1X Kinase buffer, 25 mM MgCl<sub>2</sub>, 4 mM DTT, 20 mM HEPES, pH = 7.5, 0.01 % Triton X-100). Dilute the compounds to 100X of the final desired highest inhibitor concentration in reaction by 100 % DMSO. Transfer 100  $\mu$ L of the compounds dilution to a well in a 96-well plate. The 40  $\mu$ L compound was transferred from the source plate to the new 384 well plate as an intermediate plate, and the 50 nL compound was transferred to the assay plate by Echo. Prepare a solution of ASK1 in 1x kinase buffer at 2-fold the final concentration of each reagent in the assay, and add 2.5  $\mu$ L of kinase solution to each well of the assay plate, except for control wells without enzyme (add 2.5  $\mu$ L of 1x kinase buffer instead).

Prepare substrate solution of MBP substrate and ATP in 1x kinase reaction buffer at 4-fold of the final concentration of each reagent desired in the assay. Add 2.5  $\mu$ L of substrate solution to each well of the assay plate to start reaction, shake the plate, incubate at 37 °C for 60 min, and add 5  $\mu$ L ADP-Glo reagent (Promega, USA), incubated at 37 °C for 180 min, then added 10  $\mu$ L kinase detection reagent, equilibrated at room temperature for 30 min, converts ADP into ATP and introduces luciferase and fluorescence to detect ATP. Collect data on Envision. Copy values of RLU from Envision, and convert the RLU value to a percentage inhibition value using the formula: Percent inhibition = (max – sample RLU) / (max – min) \* 100 (“min” means the RLU of no enzyme control and “max” means the RLU of DMSO control), and fit the data in the XLFit Excel add-in version 5.4.0.8 to obtain the IC<sub>50</sub> value using the formula:  $Y = \text{Bottom} + (\text{Top} - \text{Bottom}) / (1 + (\text{IC}_{50} / X)^{\text{HillSlope}})$ .

#### 4.4. Kinase selectivity experiments

Kinase selectivity experiments were determined at ICE Bioscience using the Characteristic kinase profiling platform. The compound **JT21-25** was serially diluted from 1  $\mu$ M stock in DMSO. The kinase selectivity experiment was performed using either the HTRF kinase assay or the ADP-Glo kinase assay. The method refers to the evaluation of ASK1 inhibitory activity. The readout value of reaction control (1 % DMSO) was set as a 0 % inhibition, and the readout value of background (10  $\mu$ M Positive Control) was set as a 100 % inhibition. Then the percent inhibition of each test solution was calculated as follows: % Inhibition = 100 % – (compound – positive control) / (negative control – positive control) \* 100 %. Among them, positive control represented the average data for the positive controls (10  $\mu$ M); negative control represented the average data for negative controls (1 % DMSO).

#### 4.5. Cell culture

The human hepatocyte cell lines HepG2 and LO2 were obtained from the American Type Culture Collection (ATCC, US). LO2 cells were cultured with RPMI-1640 supplemented with 10 % Fetal Bovine Serum (FBS) and 1 % Penicillin-Streptomycin (P/S). HepG2 cells were maintained in MEM supplemented with 10 % FBS and 1 % P/S. All the mentioned cells were maintained in 5 % CO<sub>2</sub> at 37 °C. The morphology and growth of the cells were evaluated under a light microscope.

#### 4.6. In vitro cytotoxicity assays

CCK-8 assay was utilized to evaluate the cytotoxicity of the highly inhibitory compound **JT21-25**. Firstly, the LO2 human normal liver cells in logarithmic growth stage were seeded into 96-well plates at a cell density of 5000 cells per well with 100  $\mu$ L of 1640 culture medium, incubated overnight. The culture medium was then replaced with fresh medium containing various concentrations of compound **JT21-25**. And **GS-4997** is used as a positive control drug. Subsequently, the cells were incubated for another 24 h and then 10  $\mu$ L CCK-8 solution was added to

per well and incubated for 1 h. Finally, the absorbance of formazan product was measured at 450 nm by a microplate reader (Multiskan FC; Thermo Fisher Scientific, USA). Untreated cells in media were used as the blank control. The process was repeated in triplicate for all treatment concentrations. The cytotoxicity was expressed as the percentage of the cell viability as compared with the blank control.

#### 4.7. hERG patch clamp assay

The HEK-293 cells stably expressing hERG channel (Catalogue: A-0320) were cultured in DMEM medium supplemented with 10 % FBS and 0.8 mg/mL G418 in culture dish. Cells grew in a humidified incubator at 37 °C with 5 % carbon dioxide. The medium was removed, and the cells were washed with PBS. Then 1 mL of TrypLE™ Express solution was added to digest the cells. The culture dish was incubated at 37 °C for 0.5 min. As soon as the cells were detached, about 5 mL of 37 °C pre-warmed complete medium was added. The solution was mixed well with pipetting up and down to break up cell clumps. Cell suspension was transferred into a sterile pipet and the cells aggregates were dissociated by gentle homogenization. Then the cell suspension was transferred into a sterile centrifuge tube and spun at approximately 1000 rpm for 5 min. The cells were maintained by seeding  $2.5 \times 10^5$  cells in a 6 cm dish (final medium volume: 5 mL) for routine maintenance. To maintain electrophysiological performances, cell density must not exceed 80 %. Before patch clamp test, the cells were detached using TrypLE™ Express solution, centrifuged by adding medium to terminate the digestion, resuspended and counted, adjusted to a cell density of  $2-3 \times 10^6$  cells/mL, and then lightly mixed with an equilibrium shaker for 15–20 min at room temperature and were tested on the QPatch. External solution was prepared as follows (pH 7.4): 140 mM NaCl, 3.5 mM KCl, 1 mM MgCl<sub>2</sub>·6H<sub>2</sub>O, 2 mM CaCl<sub>2</sub>·2H<sub>2</sub>O, 10 mM D-Glucose, 10 mM HEPES, 1.25 mM NaH<sub>2</sub>PO<sub>4</sub>·2H<sub>2</sub>O, pH = 7.4 with NaOH. Pipette Solution was prepared as follows (pH 7.2): 20 mM KCl, 115 mM K-Aspartic, 1 mM MgCl<sub>2</sub>·6H<sub>2</sub>O, 5 mM EGTA, 10 mM HEPES, 2 mM Na<sub>2</sub>-ATP, pH = 7.2 with KOH. Automated Patch Clamp system QPatch 48X (Sophion) was used for electrophysiological recording in this study. Placed the prepared cells on the centrifuge of the Qpatch work plane, washed the cells with multiple centrifugation/suspension times, and replaced the cell culture medium with extracellular solution. Took out an MTP-96 plate and placed it on the MTP source position. A QPlate chip was taken out and put in the Qplate source position. The barcode reader scans the barcode of MTP-96 board and QPlate chip and the gripper arm grabbed them to the measurement position. The intracellular and extracellular solutions from the saline reservoir were added to the intracellular saline well and cell and compound well of the QPlate chip.

For the measuring, all the measuring points of QPlate were under the initial quality control. The quality control process included sucking the cell suspension from the cell container of the centrifuge, positioning the cells on the chip hole by the pressure controller, establishing a high-resistance seal, and forming a whole-cell recording mode. Once a stable control current baseline was obtained, the test article could be applied to the cells by sequential aspiration from the MTP-96 plate in order of concentration. The hERG current was recorded using the whole-cell patch clamp technique at a holding potential of –80 mV and then depolarized to –50 mV for 0.5 s to test the leak current. Then the voltage was depolarized to 30 mV for 2.5 s. The peak tail current was induced by a repolarizing pulse to –50 mV for 4 s. This protocol was repeated at 10 s intervals to observe the effect of test article on hERG tail current. The data were collected by QPatch screening station and stored in QPatch database server. In the experiment, each drug concentration was applied twice recording period of at least 5 min. The control and test solutions were applied to the cells sequentially from low to high concentrations. During the experiment, the solutions were withdrawn from the chamber by a peristaltic pump. The current of each cell detected in the extracellular solution without compound was used as its own blank control. The assay was repeated two times independently using at least two cells

per concentration. All tests were performed at room temperature. For double applications, only the second drug application is used for data analysis. The last three data points before the next application are averaged to calculate the effect of the preceding drug application and the current values representative for test compound concentration were normalized to the reference current values as blank control ( $\frac{\text{Peak tail current}_{\text{compound}}}{\text{Peak tail current}_{\text{control}}}$ ) and the inhibition rates were calculated ( $1 - \frac{\text{Peak tail current}_{\text{compound}}}{\text{Peak tail current}_{\text{control}}}$ ). Mean, standard error (SE) and standard deviation (SD) were calculated for each test group.

$$Y = \text{Bottom} + (\text{Top} - \text{Bottom}) / (1 + 10^{((\text{LogIC}_{50} - X) * \text{HillSlope}))}$$

#### 4.8. Oil Red O staining

Oil Red O staining was applied to assess lipid droplet formation in LO2 cells. To establish the *in vitro* NAFLD cell model, LO2 cells were cultured in the presence or absence of 1 mM FFA (containing oleic acid and palmitic acid at a 2:1 vol ratio) for 24 h and used for the indicated assays.

The LO2 cells in logarithmic growth stage were seeded into a 12-well plate at a cell density of  $5 \times 10^4$  cells per well with 1 mL of 1640 culture medium, incubated overnight. Treat with 1 mM FFA, and then culture with the previously indicated concentrations (1, 4, 8  $\mu\text{M}$ ) of **JT21-25** for another 12 h. Wash the cells thrice with PBS and fix with fixing solution for 30 min. After fixation, wash thrice with double distilled water and immerse in 60 % isopropyl alcohol solution for 30 s. And then stain with Oil Red O staining solution (Solarbio, G1262) in the dark for 20 min at room temperature. After staining, wash the cell with 60 % isopropyl alcohol solution thoroughly, counterstain with Mayer's Hematoxylin Stain Solution and visualize the cells under the microscope to determine the degree of fat accumulation.

#### 4.9. Biochemical analyses and Enzyme-Linked immunosorbent assay (ELISA)

The LO2 cells were incubated and grouped according to 4.5. Oil Red O Staining At the end of incubation, cells were digested with trypsin and rinsed with normal saline for 1–2 times. Then collect the cells by centrifugation at  $860 \times g$  for 5 min. According to the manufacturer's instructions, CHOL, LDL and TG were measured by assay kits (Nanjing Jiancheng Institute of Bio Engineering, Inc., Nanjing, China), and aspartate aminotransferase (AST) serum alanine aminotransferase (ALT), were determined by automatic biochemical analyzer. (Toshiba, TBA-120 FR).

#### 4.10. Flow cytometry analysis of cell cycle distribution

The HepG2 cells in logarithmic growth stage were seeded into a 6-well plate at a cell density of  $2 \times 10^5$  cells per well with 2 mL of MEM culture medium, incubated overnight. The culture medium was then replaced with fresh medium containing compounds **GS-4997** and **JT21-25** at the concentration of 0, 0.5, 1, 2, 4, 8, and 16 mM for 24 h, respectively. And **GS-4997** is used as a positive control drug. Subsequently, all cells were collected and centrifuged at 1200 rpm for 5 min, washed twice with PBS buffer, and fixed in 1 mL of 70 % ethanol at 4 °C for 24 h. The fixed cells were centrifuged at 1200 rpm for 5 min, washed with 1 mL PBS buffer, and gently and completely re-suspended in 500  $\mu\text{L}$  of cell cycle and apoptosis Kit solution (Beyotime Biotechnology, Code C1052). The samples were incubated at 37 °C in the dark for 30 min prior to detection of red fluorescence signals at 488 nm by flow cytometry analysis (Gallios; Beckman Coulter). The data were analyzed with FlowJo software to provide to cell cycle progression status.

#### 4.11. Molecular docking

The molecular docking study of compounds **JT21-25** and **GS-4997** with ASK1 protein (PDB code: 5UOX) [33] was conducted using Discovery Studio (DS, version 4.5) and implemented through the graphical user interface DS – “CDOCKER” protocol. The three-dimensional structure of ASK1 protein in the docking study was downloaded from the Protein Data Bank (<https://www.rcsb.org/>). The energy minimization of ASK1 protein co crystalline ligands **JT21-25** and **GS-4997** was performed using CHARMM for 2000 iterations and a minimum RMS gradient of 0.01. For protein preparation, hydrogen atoms are added to remove water and impurities. After molecular docking, the interaction types between docking ASK1 protein and **JT21-25** and **GS-4997** were analyzed.

#### 4.12. In silico ADME properties

The drug-likeness, oral bioavailability, and other pharmacokinetic characteristics of **JT21-25** have been evaluated on the free web server SwissADME (<https://swissadme.ch/index.php>) [39]. Initially, the compound **JT21-25** was drawn on Marvin and the “Run!” program was executed directly on the web page.

#### CRediT authorship contribution statement

**Lidan Pang:** Methodology. **Tiantian Wang:** Writing – original draft, Resources, Funding acquisition. **Jiateng Huang:** Writing – original draft. **Jie Wang:** Methodology. **Xiang Niu:** Methodology. **Hao Fan:** Methodology. **Pingnan Wan:** Resources. **Zengtao Wang:** Writing – review & editing, Supervision, Resources, Funding acquisition, Conceptualization.

#### Declaration of competing interest

The authors declare that they have no known competing financial interests or personal relationships that could have appeared to influence the work reported in this paper.

#### Acknowledgments

This work was supported by the National Natural Science Foundation of China (NSFC, NO. 22067010), Jiangxi University of Chinese Medicine School-level Science and Technology Innovation Team Development Program (NO. CXTD22005), the General Program of Jiangxi Natural Science Foundation (NO. 20224BAB206117), the Jiangxi University of Chinese Medicine Science and Technology Innovation Team Development Program (NO. CXTD22001), the Program of Jiangxi Provincial Department of Education (NO. GJJ211234, NO. GJJ211241), the PhD Start-Up Fund of Jiangxi University of Chinese Medicine (NO. 2021BSZR024), Start-up Support Plan for Returned Chinese Students (2021 year) and Science and Technology Project of Jiangxi Provincial Health and Family Planning Commission (NO. 20185522).

#### Appendix A. Supplementary data

Supplementary data to this article can be found online at <https://doi.org/10.1016/j.bioorg.2024.107167>.

#### References

- [1] H. Ichijo, E. Nishida, K. Irie, P. ten Dijke, M. Saitoh, T. Moriguchi, M. Takagi, K. Matsumoto, K. Miyazono, Y. Gotoh, *Science* 275 (5296) (1997) 90–94.
- [2] S. Yamagishi, M. Yamada, H. Koshimizu, S. Takai, H. Hatanaka, K. Takeda, H. Ichijo, K. Shimoke, T. Ikeuchi, *J. Biochem.* 133 (6) (2003) 719–724.
- [3] T. Wang, L. Pang, M. He, Z. Wang, *Eur. J. Med. Chem.* 262 (2023) 115889.
- [4] Y. Gotoh, J.A. Cooper, *J. Biol. Chem.* 273 (28) (1998) 17477–17482.

- [5] A. Matsuzawa, H. Nishitoh, K. Tobiume, K. Takeda, H. Ichijo, *Antioxid. Redox Signal.* 4 (3) (2002) 415–425.
- [6] E. Chiang, O. Dang, K. Anderson, A. Matsuzawa, H. Ichijo, M. David, *J. Immunol.* 176 (10) (2006) 5720–5724.
- [7] K. Mizumura, Y. Gon, F. Kumasawa, A. Onose, S. Maruoka, K. Matsumoto, S. Hayashi, T. Kobayashi, S. Hashimoto, *Int. Immunopharmacol.* 10 (9) (2010) 1062–1067.
- [8] H. Nishitoh, H. Kadowaki, A. Nagai, T. Maruyama, T. Yokota, H. Fukutomi, T. Noguchi, A. Matsuzawa, K. Takeda, H. Ichijo, *Genes Dev.* 22 (11) (2008) 1451–1464.
- [9] H. Nishitoh, A. Matsuzawa, K. Tobiume, K. Saegusa, K. Takeda, K. Inoue, S. Hori, A. Kakizuka, H. Ichijo, *Genes Dev.* 16 (11) (2002) 1345–1355.
- [10] G.H. Cha, S. Kim, J. Park, E. Lee, M. Kim, S.B. Lee, J.M. Kim, J. Chung, K.S. Cho, *PNAS* 102 (29) (2005) 10345–10350.
- [11] H. Kadowaki, H. Nishitoh, F. Urano, C. Sadamitsu, A. Matsuzawa, K. Takeda, H. Masutani, J. Yodoi, Y. Urano, T. Nagano, H. Ichijo, *Cell Death Differ.* 12 (1) (2005) 19–24.
- [12] T. Nakamura, K. Kataoka, M. Fukuda, H. Nako, Y. Tokutomi, Y.F. Dong, H. Ichijo, H. Ogawa, S. Kim-Mitsuyama, *Hypertension* 54 (3) (2009) 544–551.
- [13] Y. Izumiya, S. Kim, Y. Izumi, K. Yoshida, M. Yoshiyama, A. Matsuzawa, H. Ichijo, H. Iwao, *Circ. Res.* 93 (9) (2003) 874–883.
- [14] E. Yamamoto, Y.F. Dong, K. Kataoka, T. Yamashita, Y. Tokutomi, S. Matsuba, H. Ichijo, H. Ogawa, S. Kim-Mitsuyama, *Hypertension* 52 (3) (2008) 573–580.
- [15] T. Ebrahimian, M.R. Sairam, E.L. Schiffrin, R.M. Touyz, *Am. J. Phys. Heart Circ. Phys.* 295 (4) (2008) H1481–H1488.
- [16] G. Ren, C. Huynh, K. Bijian, A.V. Cybulsky, *Mol. Immunol.* 45 (8) (2008) 2236–2246.
- [17] K. Taki, R. Shimozono, H. Kusano, N. Suzuki, K. Shinjo, H. Eda, *Life Sci.* 83 (25–26) (2008) 859–864.
- [18] Y. Hayakawa, Y. Hirata, K. Sakitani, H. Nakagawa, W. Nakata, H. Kinoshita, R. Takahashi, K. Takeda, H. Ichijo, S. Maeda, K. Koike, *Cancer Sci.* 103 (12) (2012) 2181–2185.
- [19] H.E. Tzeng, C.H. Tsai, Z.L. Chang, C.M. Su, S.W. Wang, W.L. Hwang, C.H. Tang, *Biochem. Pharmacol.* 85 (4) (2013) 531–540.
- [20] H. Ichijo, S. Maeda, H. Nakagawa, M. Nakoji, M. Takahashi, T. Shimizu, T., Osawa Nitrogen-containing heterocyclic compounds having inhibitory activity to apoptosis signal-regulating kinase, WO2012011548 (2012).
- [21] T. Fujisawa, M. Takahashi, Y. Tsukamoto, N. Yamaguchi, M. Nakoji, M. Endo, H. Kodaira, Y. Hayashi, H. Nishitoh, I. Naguro, K. Homma, H. Ichijo, *Hum. Mol. Genet.* 25 (2) (2016) 245–253.
- [22] G. Notte Preparation of N-[triazolylpyridinyl] benzamide derivatives as apoptosis signalregulating kinase inhibitors useful in the treatment of kidney disease. WO2013112741, 2013.
- [23] J.T. Liles, B.K. Corkey, G.T. Notte, G.R. Budas, E.B. Lansdon, F. Hinojosa-Kirschenbaum, S.S. Badal, M. Lee, B.E. Schultz, S. Wise, S. Pendem, M. Graupe, L. Castonguay, K.A. Koch, M.H. Wong, G.A. Papalia, D.M. French, T. Sullivan, E. G. Huntzicker, F.Y. Ma, D.J. Nikolic-Paterson, T. Altuhaifi, H. Yang, A.B. Fogo, D. G. Breckenridge, *J. Clin. Invest.* 128 (10) (2018) 4485–4500.
- [24] G.M. Chertow, P.E. Pergola, F. Chen, B.J. Kirby, J.S. Sundry, U.D. Patel, *J Am Soc Nephrol* 30 (10) (2019) 1980–1990.
- [25] J.H. Lin, J.J. Zhang, S.L. Lin, G.M. Chertow, *Nephron* 129 (1) (2015) 29–33.
- [26] R. Loomba, E. Lawitz, P.S. Mantry, S. Jayakumar, S.H. Caldwell, H. Arnold, A. M. Diehl, C.S. Djedjos, L. Han, R.P. Myers, G.M. Subramanian, J.G. McHutchison, Z.D. Goodman, N.H. Afdhal, M.R. Charlton, *Hepatology* 67 (2) (2018) 549–559.
- [27] G.R. Budas, M. Boehm, B. Kojonazarov, G. Viswanathan, X. Tian, S. Veeroju, T. Novoyatleva, F. Grimminger, F. Hinojosa-Kirschenbaum, H.A. Ghofrani, N. Weissmann, W. Seeger, J.T. Liles, R.T. Schermuly, *Am. J. Respir. Crit. Care Med.* 197 (3) (2018) 373–385.
- [28] Q.-S. Zhang, G.J. Eaton, C. Diallo, T.A. Freeman, *J. Cell. Physiol.* 231 (4) (2016) 944–953.
- [29] H. Wang, L. Pang, Y. Zhang, J. Huang, J. Wang, H. Quan, T. Wang, Z. Wang, *J. Mol. Struct.* 1290 (2023) 135954.
- [30] S. Hou, X. Yang, Y. Yang, Y. Tong, Q. Chen, B. Wan, R. Wei, T. Lu, Y. Chen, Q. Hu, *Eur. J. Med. Chem.* 220 (2021) 113482.
- [31] M. Corvaisier, J. Zhou, D. Malychева, N. Cornella, D. Chioureas, N.M. S. Gustafsson, C.A. Rosselló, S. Ayora, T. Li, K. Ekström-Holka, K. Jirstrom, L. Lindström, M. Alvarado-Kristensson, *Communications Biology* 4 (1) (2021) 767.
- [32] M.K. Himmelbauer, Z. Xin, J.H. Jones, I. Enyedy, K. King, D.J. Marcotte, P. Murugan, J.C. Santoro, T. Hesson, K. Spilker, J.L. Johnson, M.J. Luzzio, R. Gilfillan, F.-G.-L. de Turiso, *J. Med. Chem.* 62 (23) (2019) 10740–10756.
- [33] M. Lanier, J. Pickens, S.V. Bigi, E.L. Bradshaw-Pierce, A. Chambers, Z. S. Cheruvallath, D. Cole, D.R. Dougan, J. Ermolieff, T. Gibson, P. Halkowycz, A. Hirokawa, A. Ivetac, J. Miura, E. Nunez, M. Sabat, J. Tyhonas, H. Wang, X. Wang, S. Swann, *ACS Med. Chem. Lett.* 8 (3) (2017) 316–320.
- [34] S. Scarneo, P. Hughes, R. Freeze, K. Yang, J. Totzke, T. Haystead, *ACS Chem. Biol.* 17 (3) (2022) 536–544.
- [35] J. Totzke, S.A. Scarneo, K.W. Yang, T.A.J. Haystead, *Open Biol.* 10 (9) (2020) 200099.
- [36] Q. Ma, L. Gu, S. Liao, Y. Zheng, S. Zhang, Y. Cao, J. Zhang, Y. Wang, *Apoptosis* 24 (1–2) (2019) 83–94.
- [37] U. Bischoff, C. Schmidt, R. Netzer, O. Pongs, *Eur. J. Pharmacol.* 406 (3) (2000) 341–343.
- [38] E. Rubinstein, J. Camm, J. Antimicrob. Chemother. 49 (4) (2002) 593–596.
- [39] A. Daina, O. Michielin, V. Zoete, *Sci. Rep.* 7 (1) (2017) 42717.